UNIVERSITY OF CALIFORNIA,
IRVINE

Micromechanistically Modulated In Vitro Cardiomyocyte Alignment

submitted in partial satisfaction of the requirements
for the degree of

MASTER OF SCIENCE

in

Biomedical Engineering

by

Carina Jean-Tien Lee

Thesis Committee:
Professor William Tang, Chair
Assistant Professor Anna Grosberg
Assistant Professor Tim Downing

2018

CONTENTS

LIST OF FIGURES

ACKNOWLEDGEMENTS

I have been fortunate to be a member of the UCI BioMechanical Lab Group and to have Professor William C. Tang as my Master's Program advisor. During my two years of study in the UCI Master's Degree BioMedical Engineering Program, I have gained much valuable knowledge and skills. I have learned more experimental techniques and learned how to work with people from different academic backgrounds. Studying Biomedical Engineering was a big challenge for me coming from a life sciences background. A bigger challenge for me was the experience of studying abroad for the first time in my life, even though I was born in California but moved to Taiwan when I was 2 years old with my parents. However, due to the intense Master's Degree BME program at UCI, I did not have much time to miss Taiwan, my family, and friends. I have been fortunate to have Professor Tang as my advisor as he has been an excellent teacher and he has been very supportive of my work and studies. I am also grateful to the other professors (Professor Grosberg, Professor Downing and Professor Brewer) who have offered valuable suggestions and taught me new skills, also other graduate students from different labs and my undergraduates in the BME department who have helped me for allowing me to continue my research work. Professor Tang always says "A Master's student must learn how to find a problem and then find the answers to solve it." I think this phrase is a very useful motto and should be applicable for everyone no matter their academic background. I will certainly continue to keep this phrase in mind, in my future work and career.

ABSTRACT OF THE THESIS

Micromechanistically Modulated In Vitro Cardiomyocyte Alignment

By

Carina Jean-Tien Lee

Master of Science in Biomedical Engineering

University of California, Irvine 2018

Professor William Tang, Chair

According to the World Health Organization (WHO) in year 2015 alone, 18 million people died from cardiovascular-related diseases, which makes for a staggering 31% of all global deaths. Recent studies of human cardiomyocytes in-vitro have been generating scientific insights beyond traditional approaches. However, in general, human cardiomyocytes are difficult to study due to limited sample availability and due to its fragile in-vitro nature. In this work, we studied HL-1 cells, a tumor-cell derived cardiomyocyte, to ultimately quantify the relationship between cell contractility and to investigate the influence of external stimuli. The motivation behind this study was to look into cardiomyocyte contractility as a quantifiable indicator for cardiotoxicity.

We first tried to understand the implications of biomechanical cues on cardiomyocyte orientation. HL-1 cells have the ability to grow in-vitro indefinitely while maintaining the ability to rhythmically contract autonomously upon reaching confluence. We found that HL-1 cells can mimic the characteristics of human cardiomyocyte, making them an excellent candidate for proof-of-concept demonstrations. They differ from human cardiomyocyte in that they lack a natural orientation and striation in-vitro. With the success

of integrating substrates to incorporate nanoscale precision surface textures and which allow tissue engineering, the physiological environment of cells and tissues can be re-capitulated in-vitro. The purpose of this research was to align HL-1 cells on a polymer substrate to quantify their uniform contractility. We created an effective platform to observe cardiac contractility where the HL-1 cells are mechanically supported on a polymer substrate micro-machined with patterned grooves and ridges of nanoscale precision. Herein, we report on the quantitative efficiency of HL-1 cardiomyocyte alignment on various micro-patterned surfaces. The experimental results suggest that our micro-platform can promote cardiomyocyte alignment in-vitro, which is a crucial intermediate step towards rapid drug screening for cardiotoxicity.

Chapter 1 Introduction

The Bio-MEMS field is one field which adopts micro-machining and micro-fabrication technology for biomedical applications (e.g. drug delivery, tissue engineering, and in-vitro diagnostics). It can facilitate the concept such that we can study individual cell behavior from culturing which offers us with a speedy approach when compared to a more labor-intensive effort of examining the overall interaction mechanism of drugs on whole organs. The first Bio-MEMS study was reported by S.B. Carter in 1967 [1], which utilized a MEMS-based surface structure to confine individual cells in a culture to restricted areas in order to repeatedly identify and follow the cells over a long period of time. It was pointed out that Carter's method is applicable to study clone formation and time-lapse cinematography. When the advantages of using Bio-MEMS for biomedical applications became clearly apparent, there was a need to further rapidly advance the Bio-MEMS field.

The developments of the Bio-MEMS field were severely limited before the 1990s since the fabrication techniques were based on semiconductor processes and the common materials used were not bio-compatible. It was not until 1993 when Dr. George M. Whitesides introduced an inexpensive polymer polydimethylsiloxane (PDMS) microfabrication that the Bio-MEMS field was revolutionized **Error! Reference source not found.**. Due to this discovery of the bio-compatible polymer materials, the Bio-MEMS field quickly took off and started to grow rapidly at an astonishing rate. It eventually also led to the development of the field of microfluidics. Past studies have found that the advantages of the polymers were not only its bio-compatibility, but that they were also easy to fabricate and were low in cost. The most well-established and widely used polymers

today include PDMS, PMMA (polymethylmethacrylate) and negative photoresist SU-8, all of which have set the foundation for new technologies in the Bio-MEMS field.

Many Bio-MEMS-based devices have been widely developed and applied broadly in tissue engineering. Many cardiomyocyte techniques in the field of tissue engineering have been successfully developed [3]. Various platforms to study the behavior of cardiomyocytes, including contracting force, beat rate and electrophysiology have been previously reported. It appears that flexible structures and microfluidics are the most commonly used platforms. Drug screening which have been applied towards the study of the development of platforms have also been previously presented by others. However, there are several challenges in this field which need to be resolved. First, although the monitoring system can be mainly based on optical instruments, the cell force needs to be calculated from analyzed images of deformations of the cells or flexible substrates. Based on this, it is not possible to directly measure the cardiac contractile force [4][5][6][7][8][9]. Thus, the real-time information of beating frequencies and contractive forces cannot be monitored directly. Secondly, as the field-of-view in a microscope is limited, the overall device cannot be monitored under an image field without an appropriate high resolution since the cell sizes are usually of micro scale. Due to the micro size scale of the cells, a higher lens magnification is always necessary when monitoring cell morphology. However, when we use a high-resolution setting, we can only view a limited number of images at one time. It is not possible to view a large number of cells at the same time. Finally, the current methods for drug screening are very time consuming such that an overall drug discovery period can take 3 to 6 years. Based on these overall limitations, the development of a cardiac drug can take a very long time from creation to finally becoming available on the

market (Figure 1-1)

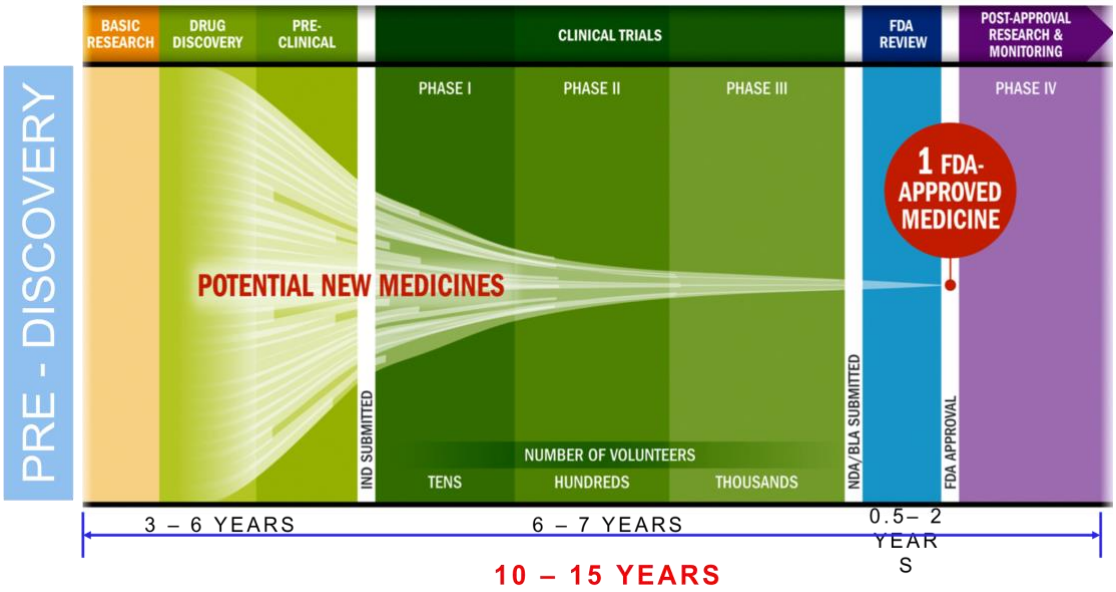

Figure 1-1. Current timeline for a new cardiac drug from development to market [10].

In this study, to better understand cardiomyocyte alignment, we developed a platform with grooves and ridges in a mechanical support system. After generating multiple PDMS devices with different surfaces, we used an UVO cleaner to treat and convert the surface of the PDMS from a hydrophobic to a hydrophilic layer. Then, fibronectin was coated on the PDMS surfaces for further cell adhesion. Finally, the HL-1 cells we used (e.g. neonatal rat cardiomyocytes) were seeded and the alignment of the cardiomyocytes were then analyzed and quantified.

1.1 Background and Current Needs for Drug Screening

In year 2009 in the United States, US$12 billion in funding was funneled through cardiac specific prescription drugs [11]. A drive in the current market has been leading the way to ensure that new drugs delivered and created are regulated so that cardiotoxicity can be

minimized. With such a growing demand for new drugs which can reduce cardio-vascular diseases, a shorter and more reliable early stage drug testing is imperative for the industry. (Figure 1-2) [12]. Therefore, it seems that there is a highly urgent real need for fabricating a MEMs device which is capable of providing instantaneous feedback regarding the level of cardiotoxicity and which can show the overall health status of current cells.

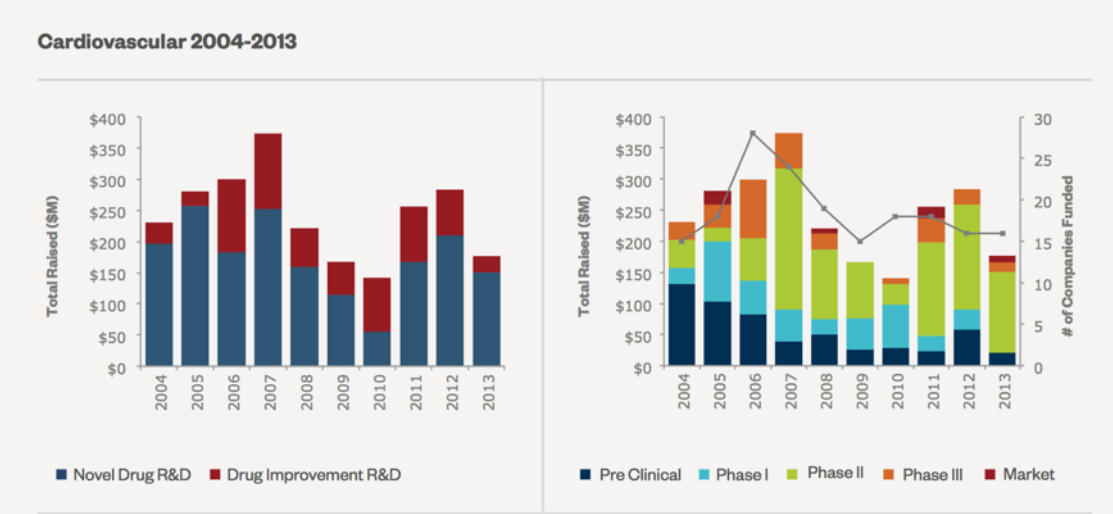

Figure 1-2. Left: Amount of venture capital funding for novel R&D cardiovascular devices over the years. Right: Venture capital investment and phase breakdown of FDA approval processes [12].

If the above limitations can be overcome, not only can it significantly reduce the lead-time for developing a new drug discovery (Figure 1-3) [10] but it can also efficiently shorten the time for bringing a new drug to market. Hence, we suggest that three necessary elements need to be introduced into a cardiomyocyte study to enable us to achieve the goal of shortening the lead-time for bringing a new drug to market. It includes massive monitoring, automatic detection and direct measurement of cardiac contractile forces (Figure 1-4).

Figure 1-3. Future timeline for a new cardiac drug to market. With the new tool development, the time span from basic research to pre-clinical phase will be reduced from 3-6 years to less than 1 year, which will shorten the time span from basic research to FDA approval to a total of 8-10 years. This is testimony of the importance of developing new drug development platforms & tools. [10].

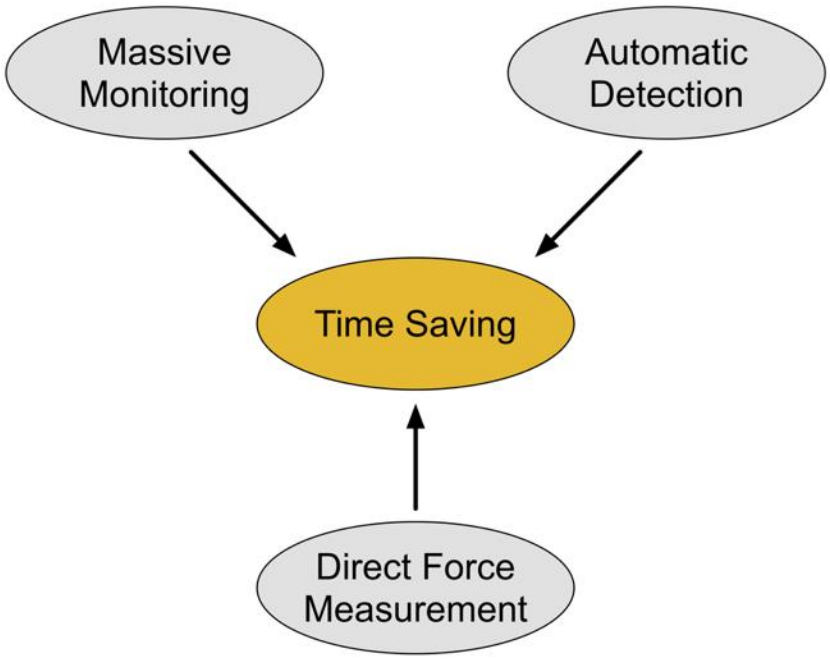

Figure 1-4. Three elements for cutting the time for bring a new potential drug to market.

1.2 Importance of Studying Cardiomyocytes

Cardio-vascular diseases (CVD) are a leading cause of death around the world. In year 2012 alone, a total of 17.5 million people died from cardio-vascular related diseases [13]. In the United States, one quarter of all deaths are CVD related which creates a high incentive for both industry and academia to focus more research work towards better understanding cardiotoxicity issues and conditions [14].

The American Heart Association reports that an estimated 83.6 million American adults have some type of cardiovascular disease. By 2030, it is projected that 44% of the US population will suffer from some form of cardiovascular disease. By 2035, over 130 million adults in the US population (45.1%) are projected to have some form of CVD, with total CVD expenditures expected to reach $1.1 trillion by 2035. This means that direct medical

costs associated with CVD is projected to reach a staggering US$748.7 billion and indirect costs estimated to reach US$368 billion. According to the statistical information from the World Health Organization (WHO) and American Heart Association (AHA), the first priority should be dealing with cardiovascular diseases. The growing rise on the dangers of cardiovascular diseases make it the number one killer each year. Unfortunately, this CVD death rate is continuing to increase year by year. We believe that there is much more needed research and study on the biomechanics of the cardiomyocytes of the heart so that we can determine how to best prevent and treat CVD. By understanding the tiny muscle cells that drive the heart, we can better understand how to control and treat heart-related diseases so that it does not kill so many people each year.

One of the difficulties in studying the biomechanics of cardiomyocytes is that the micro-environment of the cardiac tissue must be replicated. In order to better study the effect of a drug on cardiomyocytes, it is necessary to simulate the heart's native structure. In the human heart, extra-cellular matrix (ECM) fibrils naturally align to the cardiac cells [15]. We know that cell anisotropy promotes mechanical contraction and electrical propagation which result in a higher contractile force [16]. However, actual human cardiomyocytes are difficult to study due to lack of sample availability and due to the fragility of human cardiomyocytes itself. HL-1 cells offer an excellent alternative for long-term studies since they are characteristically resilient and can grow indefinitely. Most importantly, HL-1 cells can mimic the characteristics of human cardiomyocytes. In our study, we used HL-1 cells obtained from neonatal rat cardiomyocytes to study how these cells rhythmically contract autonomously after reaching confluence in-vitro and to simultaneously observe how contractility can be influenced by external stimuli. Since we know that HL-1 cells differ

from human heart cardiomyocytes in that HL-1 cells lack a natural orientation and striation in-vitro, we designed our experimental set-up to align the cells on various polymer substrates possessing different grooved patterns in a precise and continuous manner to simulate systematic contractility.

There have been many reports on methods which more closely replicate the anisotropic characteristics of cardiac tissues in-vitro and how it is used to study the biomechanics of cardiomyocytes. In this study, we chose two sets of models to study: HL-1 cells line and neonatal rat ventricular myocyte cells. The design of these models was based on improvements to techniques from previous cardiomyocyte studies.

1.3 Advantages of Micro-Fabrication

The two fabrication methods we used to create these platforms were photolithography and soft lithography (Figure1-5) [17]. The majority of the fabrication was done in a clean room environment (Figure1-6) [18] where the process conditions were precisely controlled and where we could obtain small feature sizes (≥20 μm) and with small layer thicknesses (≥5 μm). The fabrication was batch processed which allowed for multiple platforms to be fabricated at one time and required minimal use of expensive capital equipment. Soft lithography is a type of technique used for fabricating or replicating structures using elastomeric stamps, molds, and conformable photomasks. By using soft lithography, we could create many iterations of the micro-platforms with minimal expense.

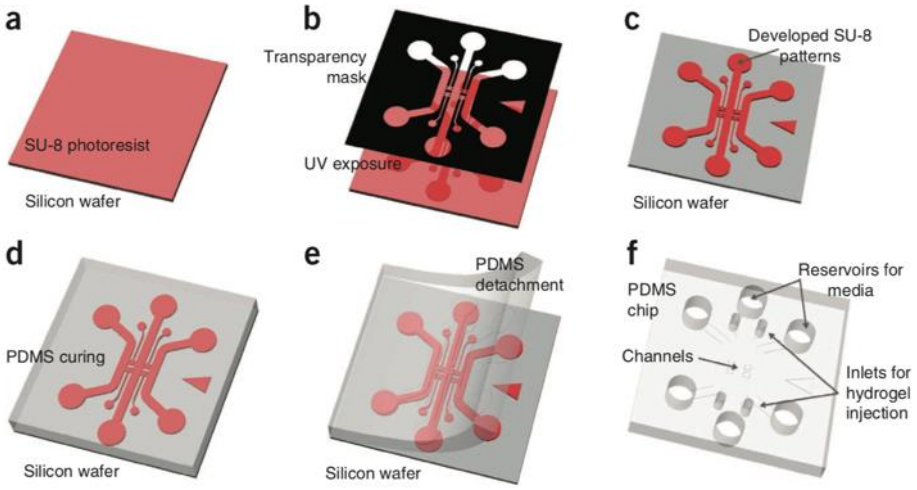

Figure 1-5. (a-f) Schematics of photolithography and soft lithography processes: (a–c) photolithography and (d-f) soft lithography. (a) SU-8 spin-coated and prebaked on a bare wafer (b) Using a transparency photomask (black), UV light is exposed on the SU-8 (c) Exposed SU-8 baked after exposure and developed to define channel patterns (d) PDMS mixed solution poured on the wafer and cured (e) Cured PDMS is peeled from the wafer (f) Device trimmed, punched and autoclaved, ready for assembly. [17]

Figure 1-6. Construction of clean-room facility specifically for soft lithography [18].

1.4 SU-8 Fabrication

We began the process by spin-coating the epoxy (SU-8) onto a silicon wafer. By using SU-

8, we could obtain feature thicknesses of 7.5um or 10um with the SU-8 Type 3005 [19].

A SU-8 epoxy was used as the cladding polymer because of its proven chemical stability, excellent optical transparency and superior planarization capacity. Before ultraviolet exposure, the SU-8 epoxy behaves like a thermoplastic polymer amenable to thermal reflow treatments and which offers the creation of a smooth surface finish, even on substrates with multi-level patterned structures. After thermal or ultraviolet cross-linking, the epoxy can become a thermosetting resin and will be robust against mechanical deformation, humidity and subsequent thermal processing. Capitalizing on the unique properties of the SU-8, we developed an ultrathin epoxy planarization process with the high degree of planarization critical to 3D photonic integration. Since the SU-8 is desirable as a material for cantilever fabrication due to its chemically inert properties, it is also a good material to use due to its transparency which allows for possible cell observation. The biggest advantage of the SU-8 is its biocompatibility [20]. Several methods in fabricating were considered and as discussed in detail later.

1.5 Soft Lithography Fabrication

The term soft lithography refers to the fabrication of patterned copies using a PDMS stamp [21]. The overall process, from pattern design to fabrication of functional structures, is generally referred to as “rapid prototyping” [22].

Due to its rapid prototyping feature, soft lithography was used in this study and we used polydimethylsiloxane (PDMS) as our substrate material.

1.6 Experimental Model

1.6.1 HL-1 Cell Line

In our study, we investigated HL-1 cells, a tumor-cell derived cardiomyocyte, to better understand the implications of biomechanics on cardiomyocyte orientation. HL-1 cells are unique in that they have the ability to grow in-vitro indefinitely while maintaining the ability to rhythmically control autonomously upon reaching confluence. These HL-1 cells mimic the characteristics of human cardiomyocytes which make them a good candidate to observe the relationship between contractility and external stimuli. However, HL-1 cells not only are derived from tumor cells and their biological properties may differ significantly from normal cells, but they also differ from human heart cardiomyocytes in that these cells lack a natural orientation and striation in-vitro.

The characteristics of the HL-1 cell contractile behavior allows for the initial testing and development using SU-8 and PDMS micro-platforms. We know that HL-1 cells can be serially passaged and stored long-term in liquid nitrogen which makes these cells easy to work with and easier to obtain than primary cells [23].

1.6.2 Neonatal Rat Ventricular Myocytes

Primary cells, which are closer to real cardiomyocytes, resemble cardiomyocyte tissue in characteristics. We used primary rat cells with PDMS micro-patterns. The primary cells were harvested from Sprague Dawley rats and C57BL/6 mice when the pups were 2 days old. These rat cells are capable of exerting a much higher contractile force than HL-1 cell line. However, in general, these rat cells are more expensive and more difficult to obtain. But, their ability to contract at higher forces make them ideal for testing the contracting characteristics with PDMS micro-patterns.

1.7 Objective and Purpose

In the study by Andrea Marquez Navarro, a previous student in our lab in 2015, the proof-of-concept of creating micro-cantilevers out of a piezoelectric material to satisfy the need of rapid feedback on cardiac conditions was presented. The system in the study of Andrea Marquez Navarro is shown in Figure 1-7.

In brief, a piezoelectric material is unique in that its mechanical deformation can create a voltage difference across the thickness of the material. If a cardiomyocyte were seeded upon a piezoelectric material, we can obtain a charge distribution as a function of the cardiac contractility and then measure it with a simple micro-voltmeter circuit analyzer. With the help of COMSOL Multiphysics (Figure 1-8), the analysis was completed in the summer of 2015 to show that with the above described scenario, the obtained voltage outputs would vary between 1-6 μV. However, that result was based on the assumption that cardiomyocyte cells contract unilaterally and uniformly. However, we know in-vitro that this is not the case. Plated cardiomyocytes experience random alignment and lack uniform contraction. To complete the design of a micro-cantilever device would then necessitate the creation of a micro-device to align the cardiomyocytes and promote uniform contraction. Prior studies have been completed by other research institutions which used electro-spun SU-8 nano-fibers to pattern and provide a mechanical support which can mimic the natural striations that in-vitro specimens exhibit [3]. This team collaborated with Dr. Madou's Bio-MEMs laboratory to design a similar device using their equipment. However, after several months of trials, the studies proved inconclusive with regards to the cell alignment.

Our group believes that the failure of the above study stemmed from three possible causes: 1) inaccuracies in the laboratory equipment which resulted in 100-200 μm specifications that were too large to facilitate structural support of the cells, 2) the cost and effort required to create one device proved too costly, and 3) the design of the device proved too difficult to prevent contaminations within the cell cultures.

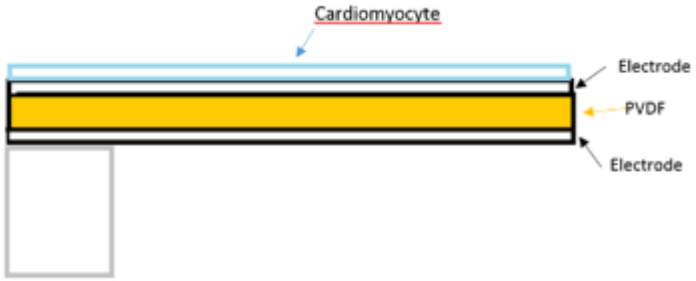

Figure 1-7. The schematically sketch of the proposed piezo-electric cardiotoxicity measurement device.

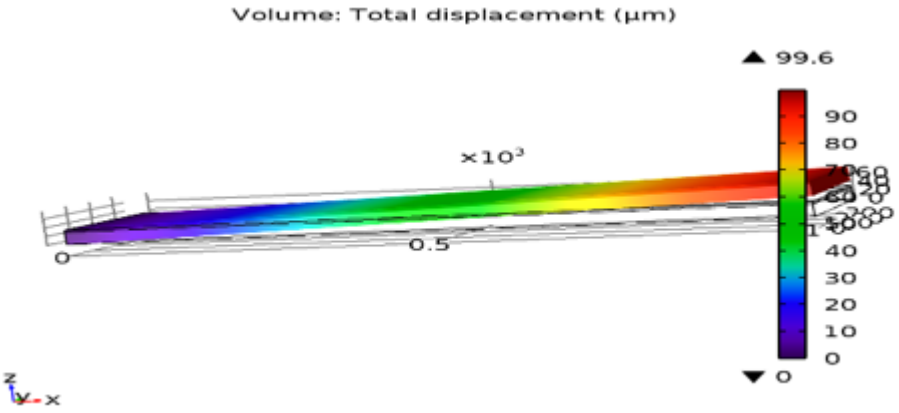

Figure 1-8. Resulting COMSOL Multiphysics showing the displacement in the z-direction on the cantilever due to the contractile forces of the cardiomyocytes with a maximum displacement of ~100 μm.

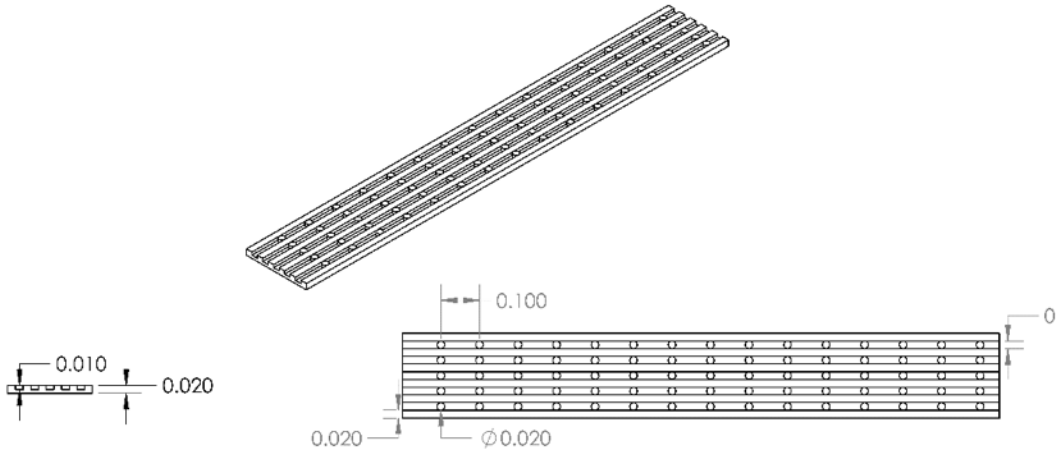

Figure 1-9. Cantilever drawing with dimensions (units: millimeters). Drawing created with SolidWorks (Dassault Systèmes)

Since then the team has moved forward to design and manufacture a novel micron-sized platform of grooves and ridges between the specifications of 5-30 μm in 10 μm increments of height and width and 10um in depth using photolithography. Details are discussed in the next chapter.

In conclusion, for initial testing, we used HL-1 cells, a tumor derived atrial cardiomyocyte line cell in our study. They were selected as they offer characteristically similar traits as normal mouse atrial heart cells. These cells show genetically similar expressions such as possessing complex a-cardiac actin and myosin heavy chains as well as structural similarities proven to be a representative of cardiac phenotypes. Further, these cells also exhibit the inability to align similar to normal cardiac cells in-vitro while exhibiting the unique characteristic of propagating indefinitely. Finally, the orientation and alignment of the cells can be studied based on the developed system.

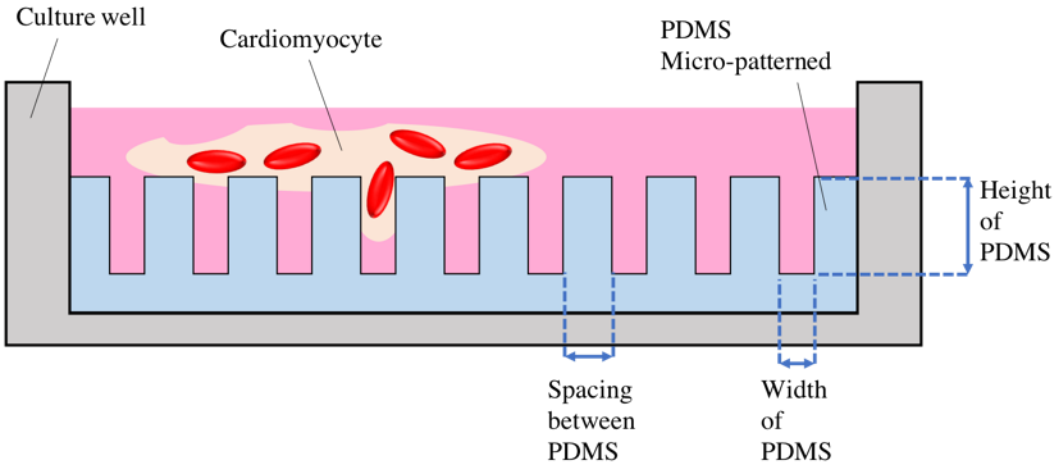

Figure 1-10. The developed system in this study

Chapter 2 Current Research Review

Biomedical research has relied on animal studies and conventional cell cultures for decades. Recently, microphysilogy systems (MPS), also known as organ-on-chips, which can recapitulate the structure and function of native tissue in-vitro, have emerged as a promising alternative [24].

2.1 Cardiomyocyte microplate platform for drug screening

A cardiomyocyte is a natural bio-electro-mechanical coupling system. To develop a system in-vitro to mimic the environment found in-vivo, it was necessary to design a system which considers the biomechanics, the anatomy, and the biomaterial compatibility. In this section, the anatomy and function of the cardiac cells and the technologies developed for cardiac drug screening are reviewed.

2.1.1 Electro-mechanical properties of cardiomyocytes

Herein, the anatomy and mechanism of cardiac cells are introduced. By studying the morphology of cardiac cells, it can provide a general method to investigate the maturation of cardiomyocytes. (Figure 2-1(A-F)) [25][26]. and its mechanism (Figure 2-1(G)) [27][28]. From this, we can better understand the function of cardiac forces. Cardiomyocytes can be seen as striated muscle constructed by a sarcomere (region between two Z lines). Typically, there are no more than two nuclei in a strip of cardiac cells and the shape of nuclei is elliptical in shape. In addition, the longitudinal axis of the nuclei will be along the oriented myofibril. An intercalated disc exists in the intercellular region where the desmosomes are expressed on the cell membrane.

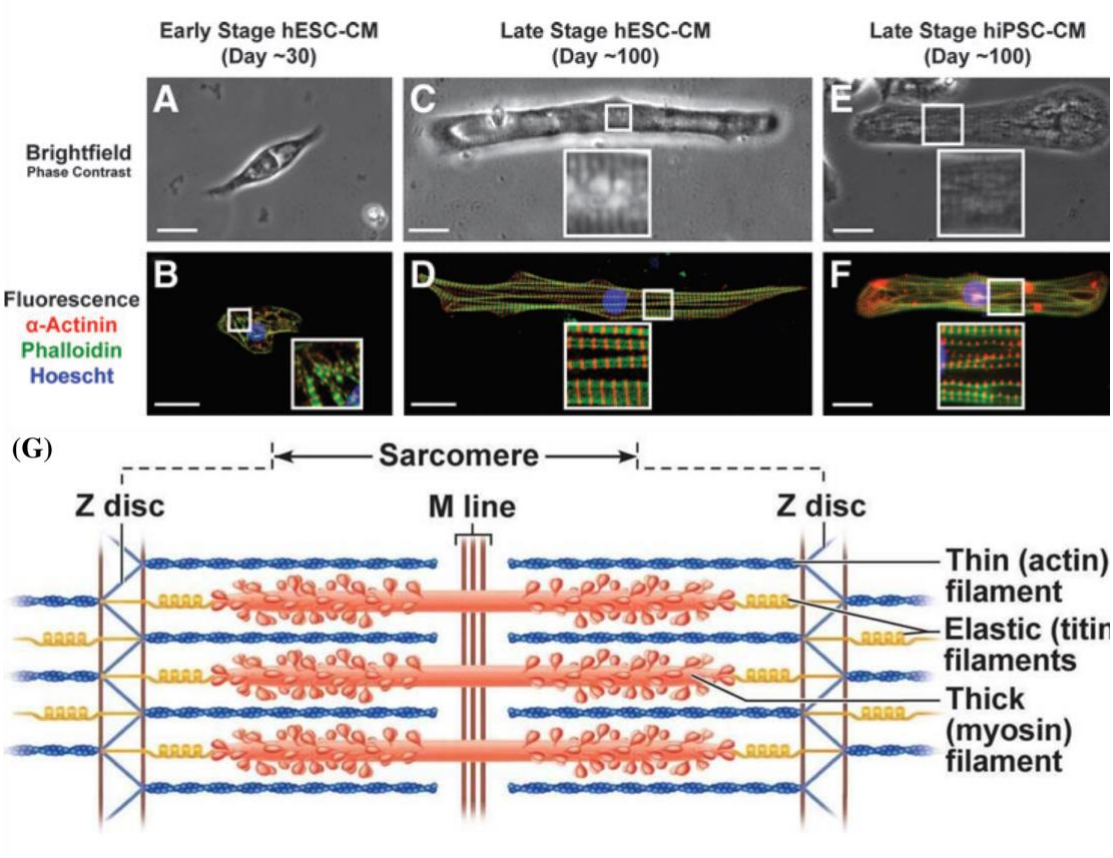

Figure 2-1. (A-F) Long-term culture induces significant changes in hESC-CM and iPSC-CM morphology. (A) By phase-contrast microscopy, early-stage hESC-CMs were round and lacked any discernable sarcomeric elements. (B) Cells at this stage were fixed and stained for α-actinin+phalloidin and showed an irregular subcellular organization and low myofibril density. (C) In contrast, late-stage hESC-CMs demonstrated sarcomeres clearly visible by phase-contrast microscopy and (D) a high degree of myofibril density, alignment, and z-disk registration. (E) Late-stage iPSC-CMs demonstrated similar enhancements by phase- contrast imaging and (F) immunocytochemistry. Scale bar 25 μm [25]. (B) Sarcomere structure [27].

The diameter of myofibril was found to range from 0.2μm to 2.3μm. The thick myofibril and thin myofibril were in parallel and formed dark, bright alternately striated bands. The bright band, called Band I, was composed of actin. The dark band called Band A was composed of myosin. There was a M line and a Z line in Band A and Band I respectively. With the mechanism of the cross-bridges formed by thick filaments with thin filaments,

the force of stroke was generated. Thus, the formation of the sarcomere is an important index for the maturation of cardiomyocytes since it can be evidenced by the maturation of the cardiac cells (Figure 2-2).

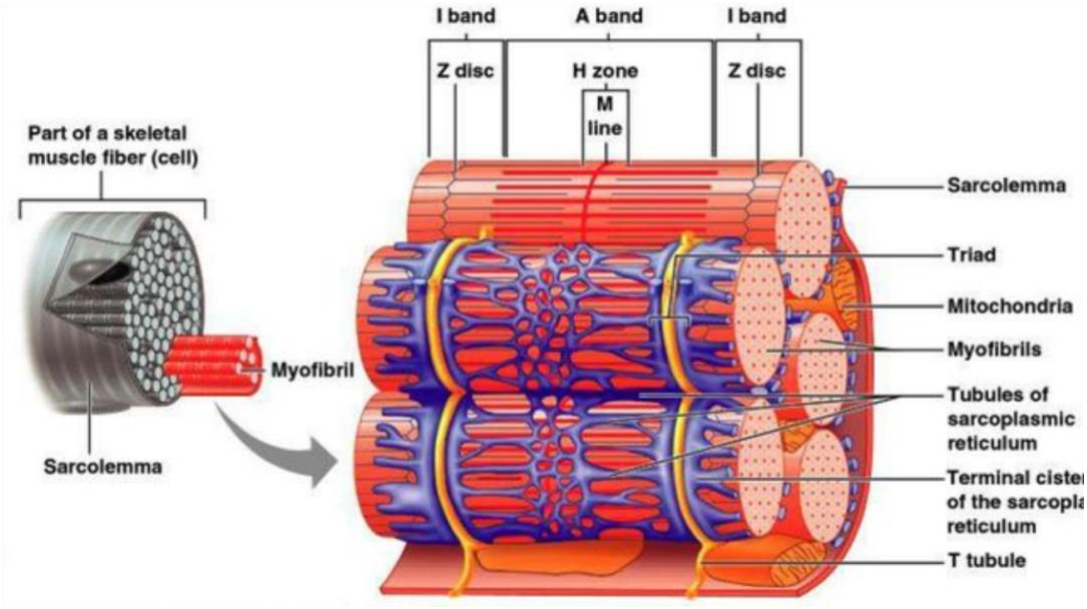

Figure 2-2. Microscopic anatomy of muscle [27].

2.1.2 Method for inducing maturation of cardiomyocytes

Cardiomyocytes, in-vitro, without any stimulation or environmental cue will not develop into mature cells without contractile function. Hence, in order to induce cellular maturation, there are three fundamental functional requirements: mechanical stimulation [25][27][29][30][31][32][33], electrical stimulation [34][35][36][37] and geometrical cue [38][39][40]. With external stimulation, cardiac cells can be promoted to reach maturation, and contractile behaviors and electrophysiological properties can be developed.

2.1.3 Mechanical stimulation

Mechanical stimulation is a method which exerts an external mechanical force to stretch the cellular scaffold and its attached cells. After mechanical stimulation, cardiomyocytes

can perform high quality adherent junctions, desmosomes, and gap junctions. From an action potential viewpoint, the performance of electrophysiology has been found to be closer to in-vivo tissues.

Zimmermann et al. [25] designed a platform that was made by putting Teflon disks or cylinders over to silicone tubing which was glued to the surface of glass culture dishes to culture circular EHTs that consist of primary cardiac cells, collagen I and other factors in the mixture. (Figure 2-3(A)). After culturing for 7 days, the engineered heart tissue (EHTs) was transferred into a tensile apparatus (Figure 2-3(B)). In the study, we used a frequency of 2Hz and a 10% cyclic stretch as the elongation mechanical stimulation for 7 more days. Figure 2-3(C) shows that the cardiomyocytes exhibited a highly mature morphology possessing a clear sarcomere with branches of muscle bundles, with cell bundles mainly consisting of longitudinally oriented cardiac myocytes with sarcomeres. The results indicate that the EHTs represent highly differentiated cardiac tissue constructs, making EHTs a promising material for in vitro studies of cardiac function and tissue replacement therapy.

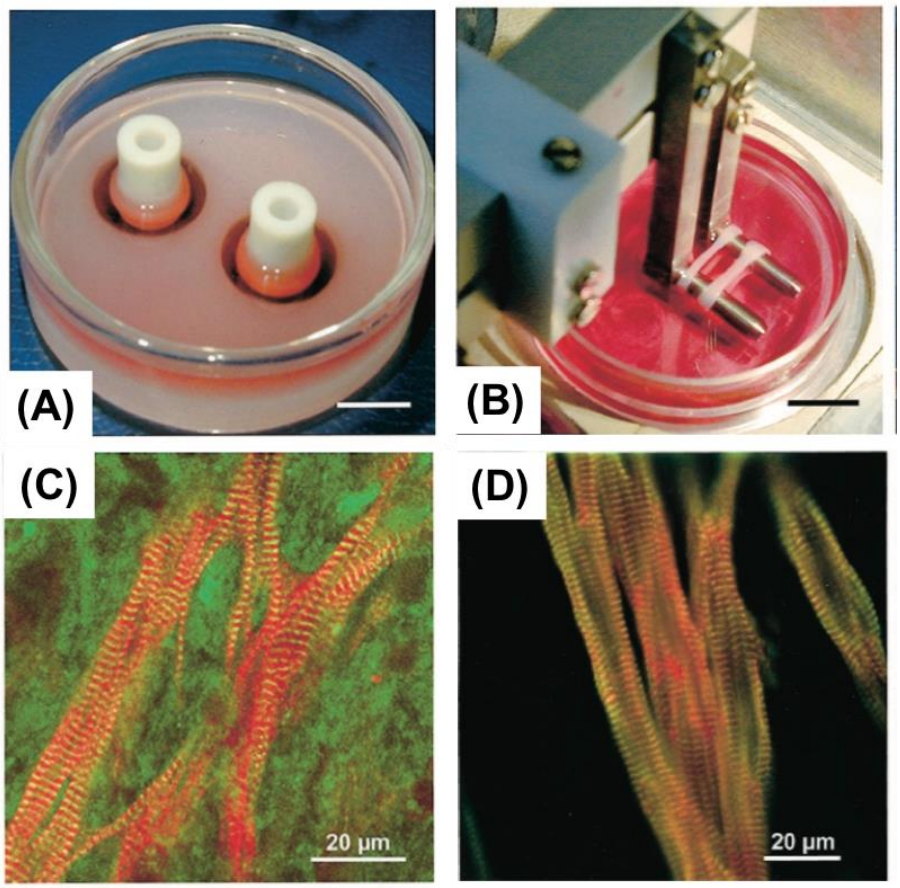

Figure 2-3. (A) Experimental set up (B) Tensile apparatus (C-D) Mature cardiomyocyte, show that actin appears as red; myomesin as green; and actinin as green [25].

2.1.4 Geometrical inducement

The cardiac cells were first anchored onto the substrates and allowed to adapt to its environment, before the mechanical and electrical stimulations were carried out. If the physiological environment is not suitable for cells, the cardiac cell may go into apoptosis. Thus, to study the morphology of cardiac cells and to stimulate cardiomyocyte growth, we needed to design a suitable substrate.

Kim *et al*. [40] fabricated a micro-groove on a flat surface of micro-cantilevers (Figure 2-4). Using a micro-grooved cantilever, the three-dimensional structures were created and

the cardiac cells were guided to align along the microstructures. As the fluorescent images Figure 2-5, the cells possessed a more matured morphology on the grooved structure than on the flat surface. The F-actin and nuclei are shown parallel to the grooves. In contrast, they were found to perform isotropically on a flat substrate.

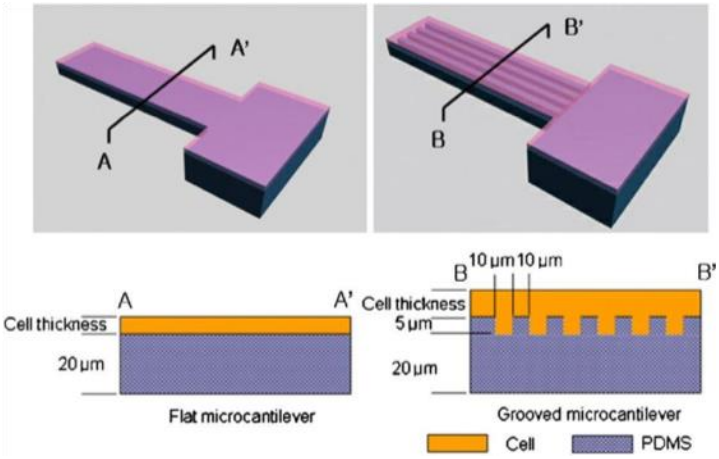

Figure 2-4. Schematics of a cross-section of a 3D hybrid biopolymer micro-cantilever structure: (left) flat microcantilever and (right) grooved micro-cantilever [40].

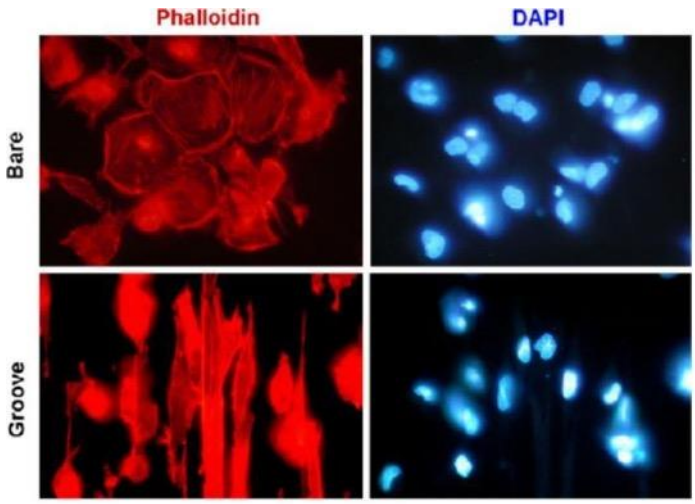

Figure 2-5. Cells stained with Phalloidin and DAPI on the flat and grooved substrates [40].

Adam W. Feinberg, *et al* [41] fabricated micro-patterned surfaces which were used to build a 2-dimensional myocardium, along with parallel arrays of multi-cellular myocardial fibers to test the effect of alignment on contractile function and muscle physiology. The results can be seen in Figure 2-6. They reported that by increasing the peak systolic stress in engineered cardiac tissues, it corresponds to an increase in the sarcomere alignment.

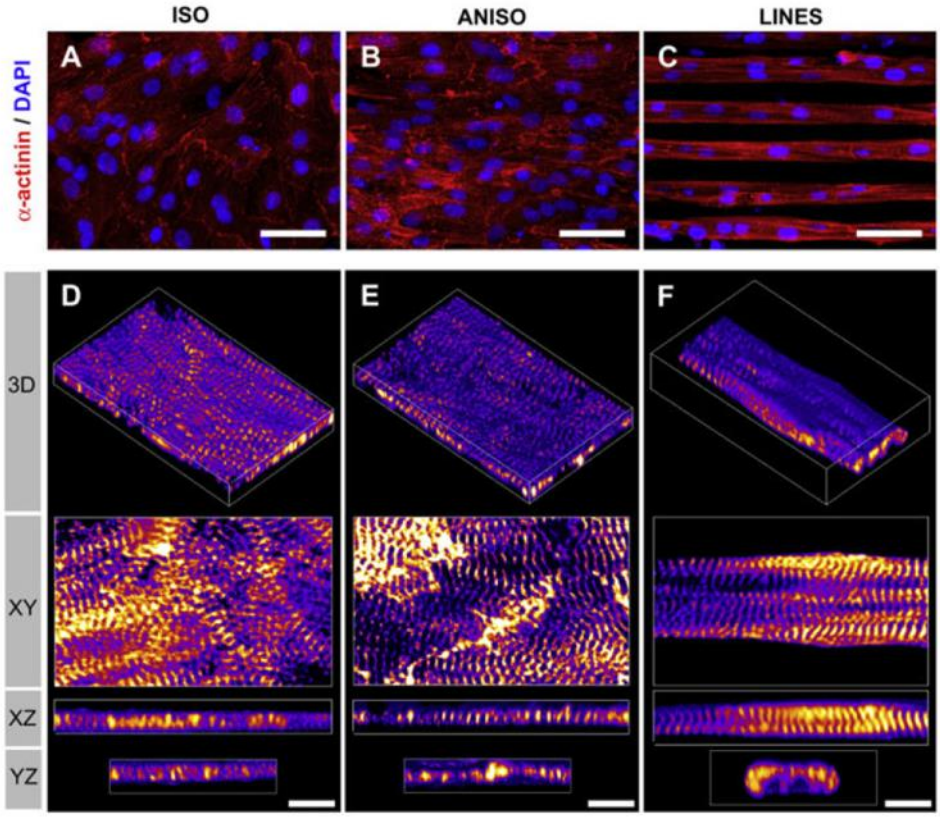

Figure 2-6. (A and D) ISO characterized by myofibrils oriented in all directions. (B and E) ANISO characterized by a predominantly uniaxial myofibrillar alignment, but with clear orientation off-axis as well. (C and F) LINES have uniaxial myofibrillar alignment.

Frances Y. *et al* [42] used a micro-patterning approach to have straight control of the macrophage cell shape (Figure 2-7(A)). Demonstration of the elongation itself without the exogenous cytokines led to the expression of the M2 phenotype markers and reduced the

secretion of the inflammatory cytokines. The alterations in the cell shape were associated with changes in the ECM architecture which can provide integral cues to modulate the macrophage phenotype polarization (see Figure 2-7(B)).

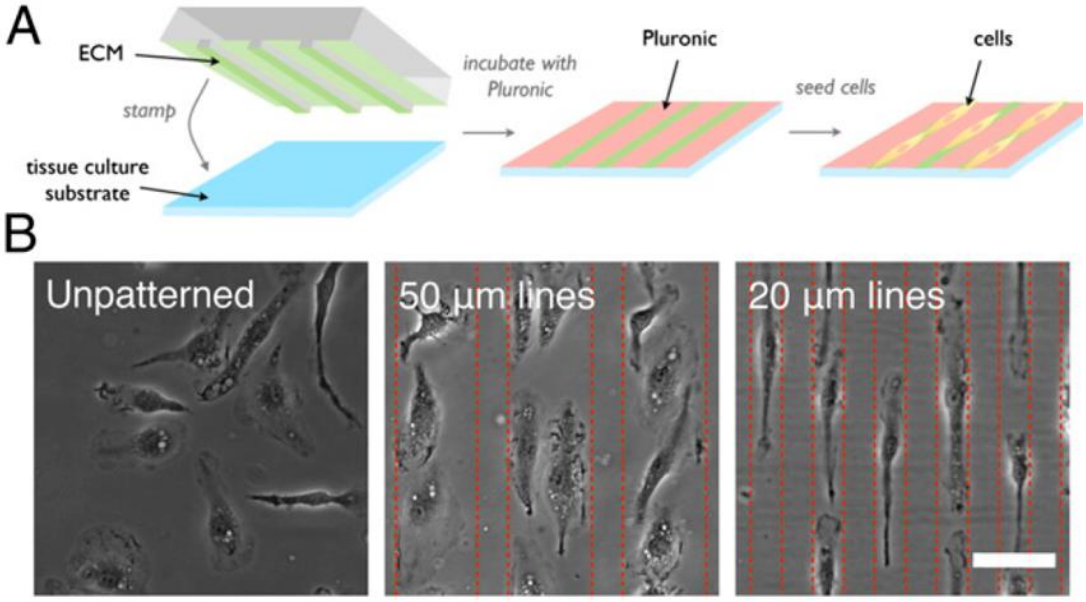

Figure 2-7. Elongation of cells by micro-patterning drive macrophage polarization. (A) Schematic of method used to micro-pattern cells by micro contact printing of arrays of fibronectin lines of various widths. (B) Phase contrast images of non-patterned cells and cells patterned on 50µm and 20µm width lines. (Scale bar: 50 µm) [42]

Apart from inducing cardiac cells to have a 3D structure, *Xiao et al*. [38][39], designed a micro-fabricated bioreactor to generate 3D micro-tissues, called bio-wires, to serve as a drug screening platform (Figure 2-8). The geometry of the suture was found to induce the cardiac cells to align along the axis of the suture and form a cell monolayer (Figure 2-9(A)). Figure 2-9(B) demonstrates that with the use of the bio-wire, most of the cells aligned along the longitudinal axis when compared to the control group.

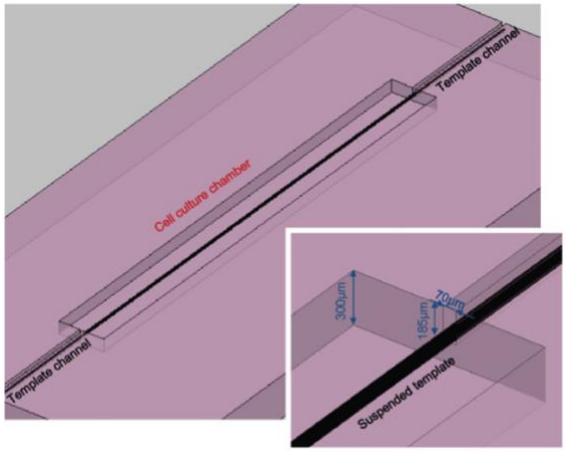

Figure 2-8. Device design of the micro-fabricated bioreactor with a suspended 6-0 suture template [38].

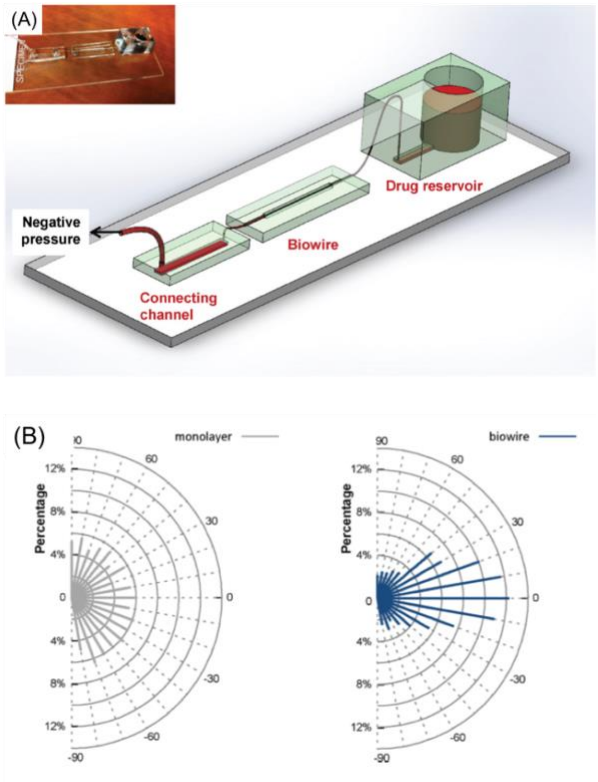

Figure 2-9. (A) Device design of the micro-fabricated bioreactor with a suspended 6-0 suture template. (B) Characterization of nucleus orientation reveals random distribution of nuclei in the monolayer group (random direction as 0 degree) and oriented distribution of the nuclei along with the suture template in the biowire group (orientation of suture template as 0 degree) [38].

Chapter 3 DEVICE ENGINEERING

3.1 Introduction

The SU-8 mold in our study was made using a photomask which was first designed on a silicon wafer using AutoCAD, then fabricated in a clean room. The micro-patterned devices were then fabricated using a PDMS material. The main advantage of using PDMS is its lower elastic modulus. The micro-cantilevers are also more flexible making it easier to see cardiomyocyte contraction for further cantilever bending. In addition, since the contraction from the cardiomyocytes can be measured by the displacement of the cantilevers optically, the PDMS micro-patterns appear to be more sensitive to cardiomyocyte contraction.

This chapter describes the fabrication protocols used to create the micro-platforms.

3.2 Micro-Platform Design

Photolithography offers us the ability to manufacture and reproduce the desired design of the micron grooves and ridges at a low cost. With knowledge that an average cardiomyocyte diameter ranges from 15μm to 20μm, we wanted to see if creating the devices could support the structures sufficiently for alignment and at what required parameters for the support to obtain sufficient alignment. To do this, we designed six different substrate pattern sizes: 5μm, 10μm, 15μm, 20μm, 30μm, and, 50μm in both width and spacing of ridges (see Figure 3-1 and Figure 3-2).

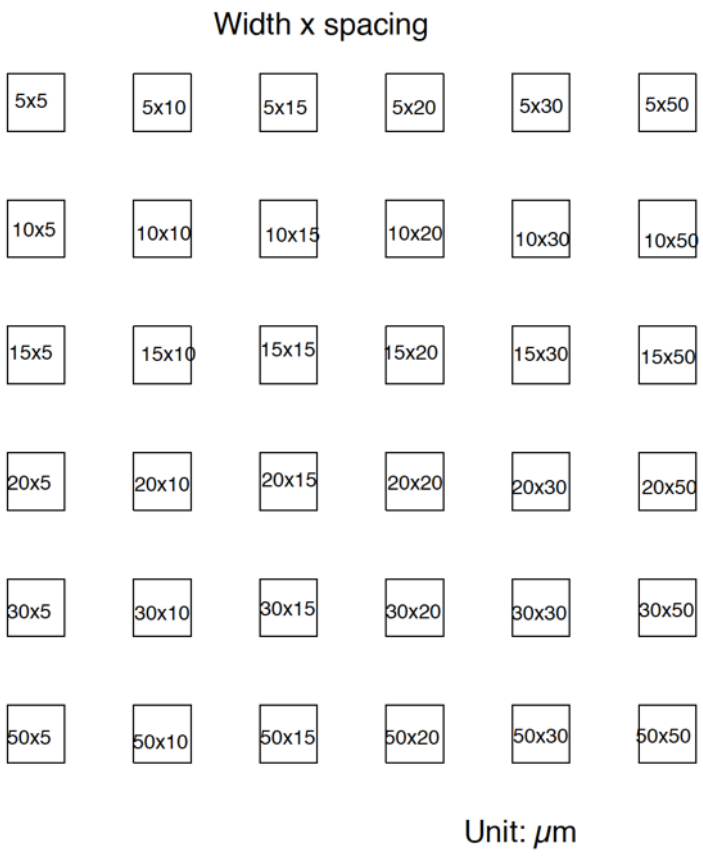

Figure 3-1. Displays the engineering diagram for the created micro-platforms (notice the increasing width and separation between each groove/ridge that allows for the quantification of the best mechanical support for the cardiomyocytes).

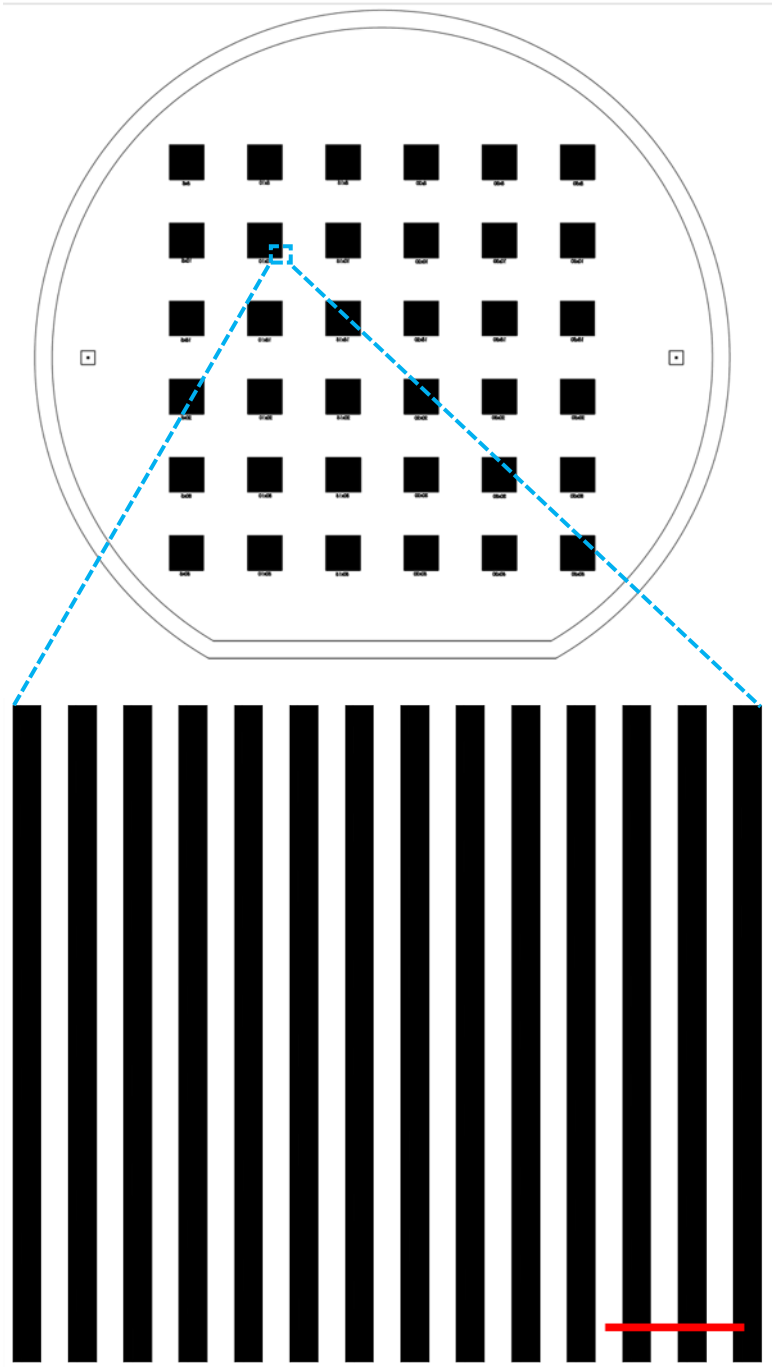

Figure 3-2. Diagram of the photomask design. (top left corner is 5µm x 5µm, bottom right corner is 50µm x 50µm; this figure corresponds to Figure 3). Zoomed in view of the 10µm x 10µm micro-pattern. (Scale: 50 µm)

3.3 SU-8 Mold Fabrication

The photomasks were designed on AutoCAD so that we could achieve dark width lines of 5µm, 10µm, 15µm, 20µm, 30µm and 50µm, resulting in grooves on the SU-8 mold. The processes of photolithography are listed below. Figure 5 shows the SU-8 photolithography process. First, a four-inch silicon wafer (University Wafer) was dipped in a 2% hydrofluoric-acid (HF) solution for 2 minutes to remove the surface oxide layer, rinsed with DI water and then dehydrated on a hotplate. We followed the recommended processing guidelines from MicroChem for our patterns.

There are two different SU-8 design used in our study, 10µm and 7.5µm. A layer of 10 (7.5) micron thick SU-8 3005 was spin-coated onto the wafer at 1000 (2000) rpm for 30 seconds. After a 3-minute soft bake on a 95 °C hotplate, the wafer was put into a Karl Suss Ma6 mask aligner (SÜSS MICROTEC SE) to expose for 20 (17) seconds at 10 mJ/cm^2 lamp conditions. A post exposure bake was carried out for 2 (1.5) minutes on a 95 °C hotplate. Afterwards, the wafer was developed in the SU-8 developer for 3 (2.5) minutes and rinsed, then dried.

3.3.1 Silicon Wafer treating

Before starting the actual fabrication, proper cleaning needed to be performed correctly. If proper cleanliness is not managed well, it can affect the surface performance and the success of the experimental work. Therefore, in order to obtain maximum process reliability, substrates should be clean and dry prior to applying the SU-8 3000 resist.

Diluted hydrofluoric acid (HF) was used to remove the native silicon dioxide from the wafers. A 2% HF was created by pouring 480 mL of DI water into 20 mL of 49% HF in a propylene beaker. The wafers were soaked for 1-2 minutes in the 2% HF solution.

After soaking, the wafer was rinsed with DI water and a wetting test performed to test for hydrophobicity. Since the oxide was hydrophilic and silicon was hydrophobic, if the water beaded up and rolled off the surface, it was considered clean of oxides. The wafer was then dried with nitrogen gas and ready to pattern the photoresist.

3.3.2 Pattern Photoresist

SU-8 3000 was used in this photolithography. The SU-8 3000 is a permanent epoxy negative photoresist with a high contrast feature. Two different parameters of heights of SU-8 were created: one is 7.5μm and the other was 10μm. The 7.5μm height one was made with an exposure energy of 10 mJ/cm^2 for 17 seconds, while the 10μm was made with an exposure energy of 10 mJ/cm^2 for 20 seconds. The wafers were then developed using the SU-8 developer and post exposure baked. The results of the fabrication for these micro-patterned are described later in the chapter.

3.3.3 Hard bake

The purpose of hard baking after development is not only to anneal and strengthen the SU-8 but also to allow the SU-8 to have better adhesion and to expand the lifespan of the master mold. This hard baking process helps to reduce cracking of the SU-8 mold. After the SU-8 has been developed, the wafer was placed on a hot plate and the temperature was slowly increased, then cooled down, then let stand for 10 to 20 minutes between each interval after the hotplate reached the specified temperature. The temperatures used were 65 °C, 90 °C, 120 °C, 150 °C, 120 °C, 90 °C, and finally 65 °C. After the final 65 °C interval at 20 minutes, the hot plate was turned off and the wafer was cooled to room temperature to avoid cracking.

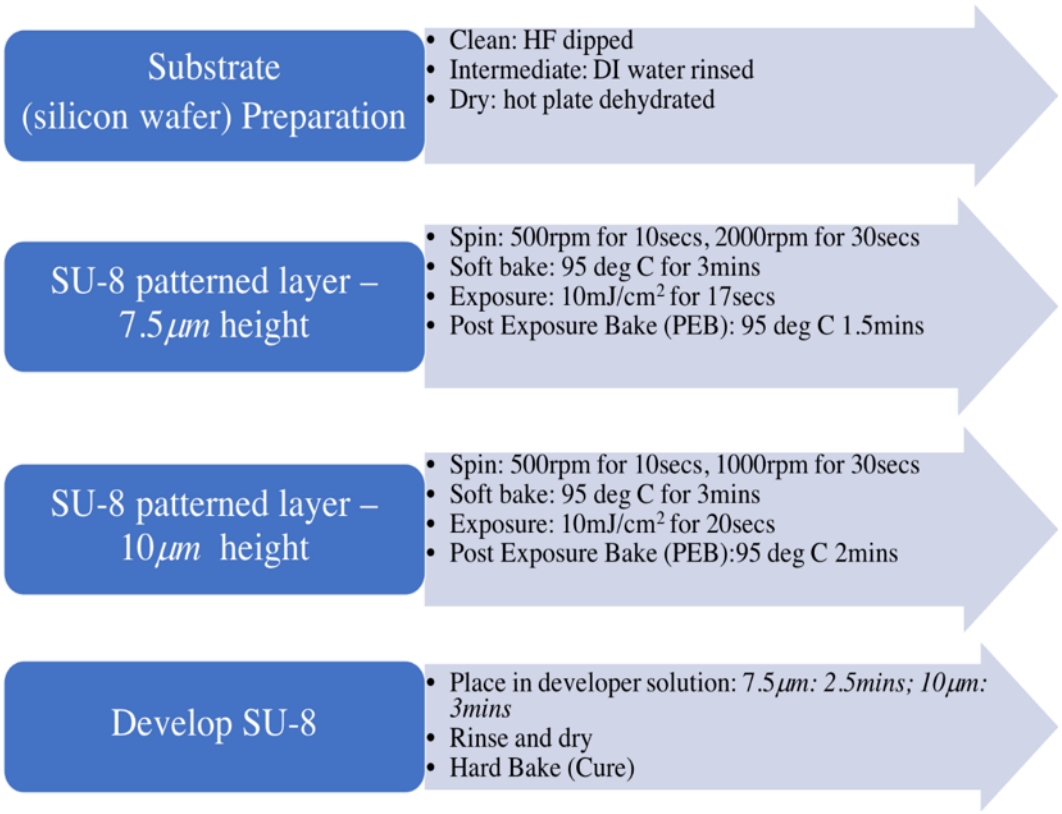

Figure 3-3. SU-8 Micro-patterned fabrication process.

3.4 Lithography: Fabrication of PDMS Micro-Patterns

Schematic of PDMS platform is shown in Figure4-5. The micro-pattern platforms used in this study were made out of PDMS material. Each platform was made using a silicon elastomer base (Sylgard 184, Dow Corning) mixed with a cross-linker (Sylgard 184, Dow Corning) at a ratio of 10:1 by weight. Our process was as follow:

1. Pit a plastic cup on the scale and zero the scale (in grams).
2. Spoon the desired amount of elastomer base into the cup and note the weight.
3. Carefully pour the curing agent (located in a small squeeze bottle) into the cup while on the scale.
4. Turn off scale.

5. Use a plastic knife and mix vigorously for 10 minutes until PDMS is white and foamy.
6. Place the cup into the desiccator vacuum to remove all bubbles (about 30 minutes).
    a. Open the vacuum valve on the wall and turn on the desiccator valve (line parallel to the tub indicates the valve is open)
    b. When the vacuum is on, you should not be able to lift the desiccator top off
    c. Evacuate the desiccator and turn the valve off (the foam will start rising).
    d. Pop the bubbles by purging with a burst of air (turn valve quickly to open and then close quickly)

After completing the above steps, the PDMS was poured on the mold. Put the mold back into the vacuum jar to remove any bubbles introduced while pouring. The thickness for this platform section is not too important. However, in order to get better resolution when imaging, the platform should be approximately 1mm-2mm in thickness. Before placing the mold in a 65 °C oven, check to make sure there are no air bubbles on the surface (note: also check the level inside the oven; let the mold cure in an oven for at least 4 hours.). After curing, the cross-linked PDMS on the mold can be cut with a surgical blade and peeled off from the mold.

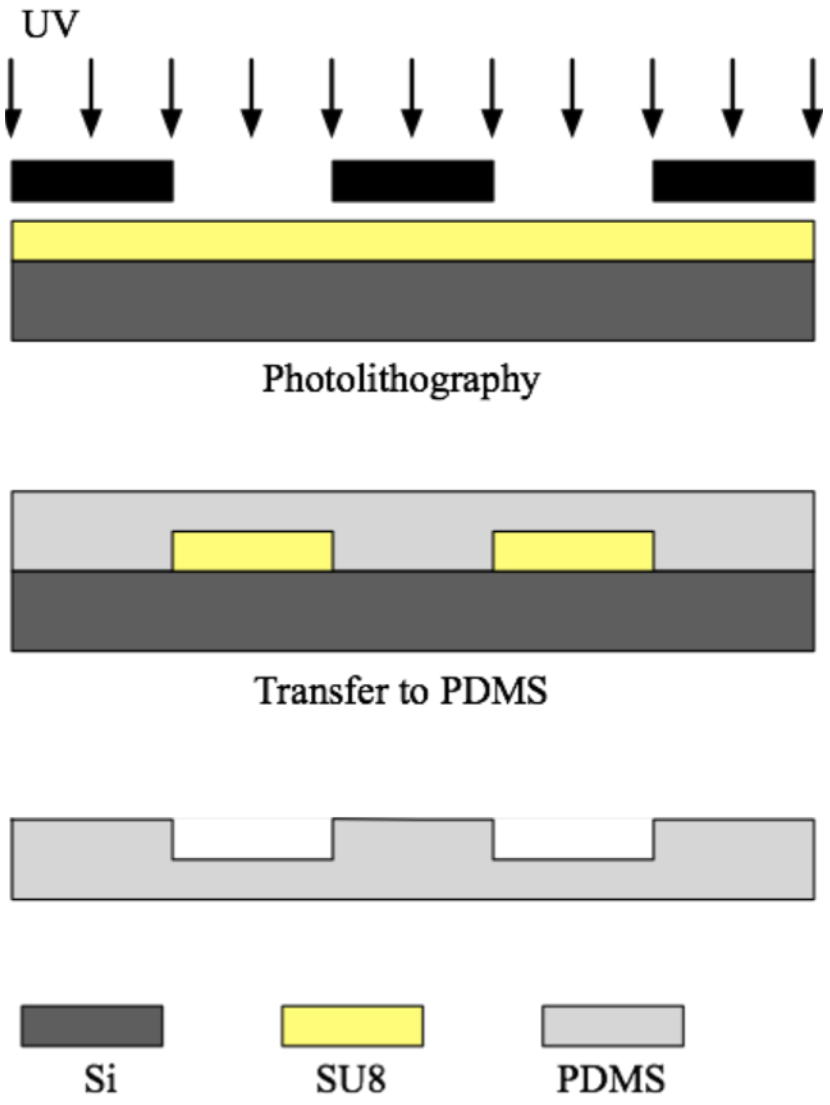

Figure 3-4. Schematic of PDMS platform

Chapter 4 EXPERIMENTAL APPROACHES AND RESULTS

4.1 Material and method

The cardiomyocyte experimental methods will be discussed in this section

4.2 Introduction

Once the fabrication process of the SU-8 fabrication and PDMS micro-platforms were developed, we fabricated several micro-platforms for experimentation with the cardiomyocytes. First, the HL-1 cardiomyocytes and the primary neonatal rat ventricular myocyte (NRVM) cells were cultured on the micro-patterned PDMS surfaces. In this chapter, the cell culturing protocols for the HL-1 cells and primary cells are discussed and the experimental results from seeding the cardiomyocytes on the micro-patterned PDMS are presented.

The HL-1 cardiomyocyte cell line was used for the initial cell experiments on the PDMS micro-platforms due to the cell line's ability to be indefinitely passaged and stored. In addition, PDMS platforms are cost effective and can show spontaneous contractile [43]. However, as HL-1 cell lines can proliferate easily, it can be an issue as real cardiomyocyte cells do not [44]. Also, since a NRVM cell ceases to proliferate after birth, we used primary rat cells for our further study. In addition to NRVM cells being closer to a real cardiomyocyte, Alford et al reported primary neonatal rat cardiomyocytes have a peak systolic stress of 9.2 kPa, which is much higher than the 1- 2 kPa HL-1 cells which are capable of generating [45][46].

4.3 Device preparation for cardiomyocyte culturing

Before seeding the cardiomyocytes onto the designed micro-patterned PDMS devices, all the devices were autoclaved as part of the sterilization procedure. After sterilization, the devices were put into an oven to dry. Then, we used an ultraviolet ozone cleaner (UVO cleaner) (Jelight Company) to automatically clean and improve the coating adhesion as well as performing surface treatment to convert the PDMS surface from a hydrophobic to a hydrophilic one (see Figure 4-1). We then added a gelatin/fibronectin solution (Sigma-Aldrich) (composed of a concentration of 200 ppm gelatin and 5 ppm fibronectin) into a flask tissue culture wall to cover the PDMS surface which had been pre-coated with the fibronectin. The PDMS was then incubated at 37 °C for at least an hour. All of these preparation processes were done before the cell thawing and seeding. Once the coating step was ready, we aspirated the gelatin/fibronectin solution, calculated the cells concentrations, then seeded the cardiomyocytes.

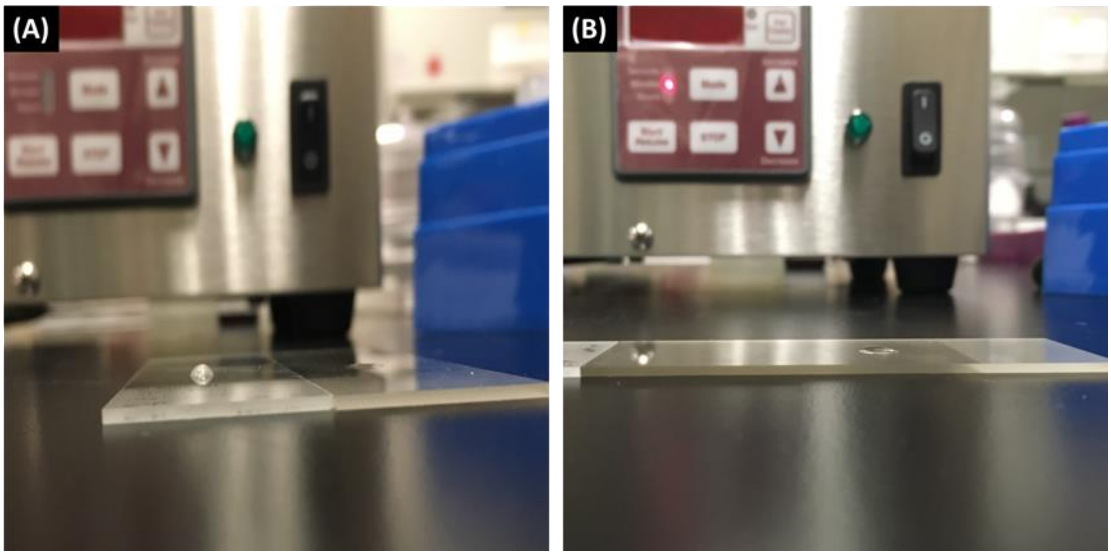

Figure 4-1. Water drop on the surface of the slide after application with UVO cleaner. (A) Before treatment, the PDMS surface was hydrophobic. (B) After treatment, the PDMS surface became hydrophilic.

4.3.1 Cardiomyocyte seeding

We used HL-1 cardiac muscle cells ($\geq 1X10^6$ cells/vial) from Sigma-Alrich (Catalog No. SCC065). For all the HL-1 cells cultured in our work, we adhered to and followed the commercially recommended protocol as below.

First, a vial of HL-1 cells was taken out from a liquid nitrogen tank. We waited until the frost melted before immediately putting into a vial pre-warmed in a 37 °C water bath for 2 minutes. Secondly, the cells were pipetted and transferred into a 15ml centrifuge tube which contained a wash medium (Claycomb medium containing only 5% FBS and penicillin/streptomycin). Then, it was centrifuged at 5 minutes at 500g. Meanwhile, we removed the gelatin/fibronectin solution from each device, and added a supplemental Claycomb medium to cover the devices. We then set it aside. We then removed the tube from the aspiration and removed the wash medium by aspiration. After removing the

supernatant, we gently re-suspended the pellet in the supplemental Claycomb medium, then seeded into each device and incubated inside a 37 °C, 5% CO_2 incubator for 4 hours to allow for the cell adhesion. After that, the unattached cells were removed and the media was changed with a pre-warmed media including all the required growth factors. The complete supplemental Claycomb media contained the following components: 87% Claycomb medium, 10% fetal bovine serum, 1% penicillin/streptomycin, 1% norepinephrine, and 1% L-Glutamine.

4.3.2 HL-1 cardiomyocyte culture

Based on the recommended protocol, the media was changed daily in order to discard any dead cells. We included a pre-warming process and washed the cells twice before adding fresh medium. In this study, we cultured HL-1 cells for 3 days, and fixed the cells on Day 3 after imaging.

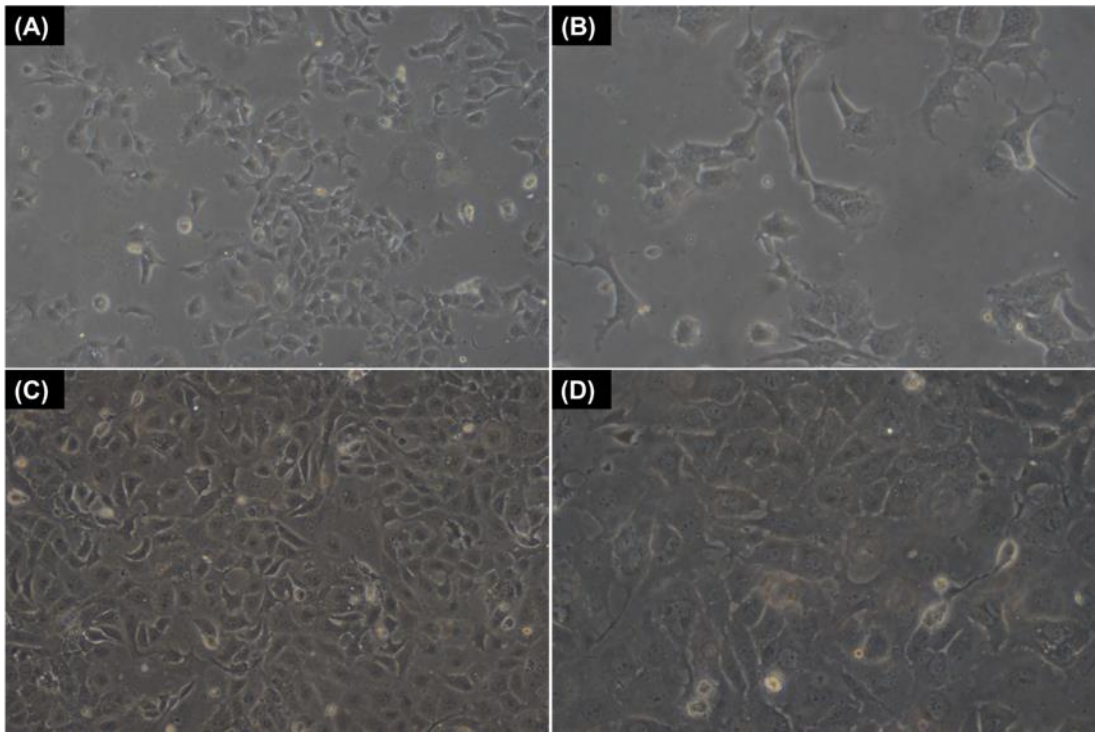

Figure 4-2. HL-1 cardiomyocytes. (A-B) Culture after Day 1, (A) 10X magnification, (B) 20X magnification. (C-D) Culture after Day 3. (C)10X magnification, (D) 20X magnification. Photos show the cells aggregating.

4.3.3 Neonatal Rat Ventricular Myocytes (NRVM) culture

Some primary cells, Neonatal Rat Ventricular Myocytes, were obtained from Dr. Grosberg's Lab. The cells were already isolated and were placed in a 15ml centrifuge tube with a complete medium. Back in our lab, the cells were seeded on our gelatin fibronectin-coated PDMS devices. All the devices were incubated in a standard 37 °C, 5% CO_2 incubator. We changed the medium daily. Starting from Day 2, the cells were fed every other day and the medium was change to a 2% fetal bovine serum culture medium. The completed medium contained the following components: 87% medium 199 (Thermofisher), 1% HEPES buffer solution (Thermofisher), 1% MEM non-essential amino acids (Thermofisher), 1% L-glutamine (Thermofisher), 20% glucose solubilizer, 0.02% vitamin

B12/penicillin solution (Sigma), and 10% heat-inactivated fetal bovine serum (Sigma). In our 2% culture medium, all the growth factors were added except for the 2% fetal bovine serum.

The other primary cells were harvested from C57BL/6 mice which were raised by Dr. Brewer. We followed the same protocols as the one we used for the NRVM cell culturing. Two 2-day-old mice were used for each experiment. After the mice were dissected, the mice hearts were quickly removed and put into a chilled dissociation buffer (1X HBSS) (Gibco). The ventricles were cut into 1mm to 2mm cubes and dissociated by alternating treatments at 4 °C with a solution of trypsin/HBSS overnight.

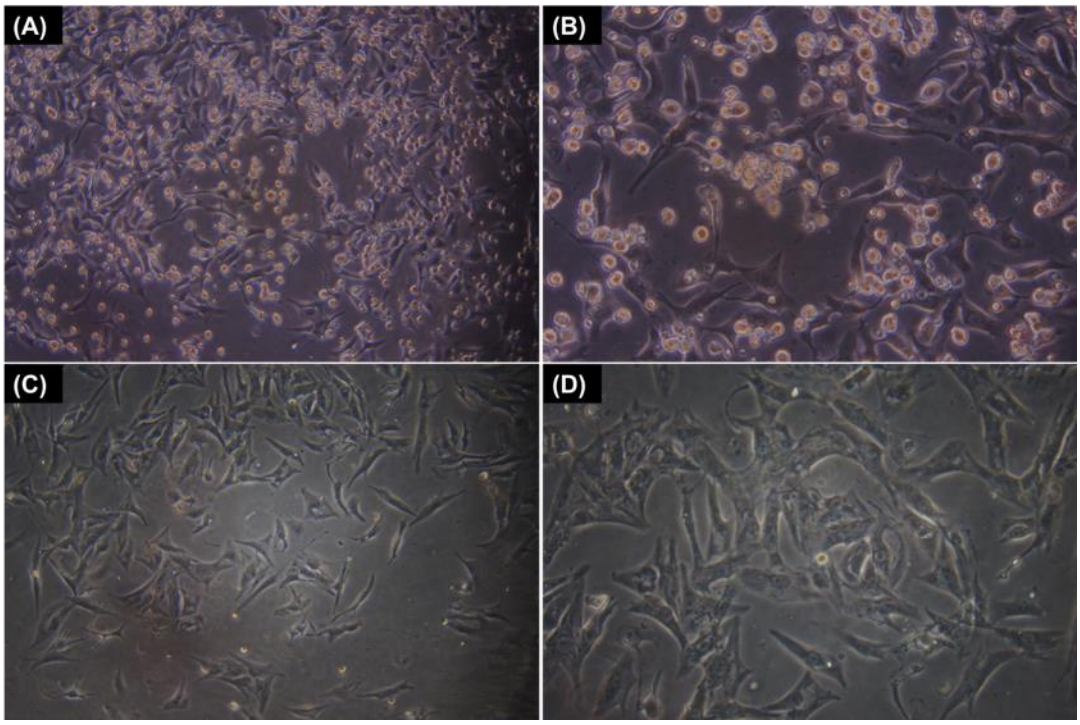

Figure 4-3. Neonatal rat ventricular myocyte (NRVM) cells. (A-B) Culture after Day 1, (A) 10X magnification, (B) 20X magnification. (C-D) Culture after Day 3, (C)10X magnification, (D) 20X magnification. Photos show cells aggregating.

4.4 Alignment study

The experimental set-up is shown in Figure 3-4. The method we used for our micro-line tissue engineering study was captured with a SONY and Nikon digital camera attached to an Olympus IX51 inverted microscope. The patterned grooves from the bright field images were aligned vertically. We continued with culturing and imaging for 3 days.

Process of cell fixing

We used the following steps to fix the cells:

1. Rinsed the cells three times with a warmed 1X PBS.
2. After the 3rd PBS wash, aspirated the PBS and replaced with a 2mL 4% Paraformaldehyde (PFA) (Sigma)+ 1 μm Triton-X 100 (Sigma) per device for 10 minutes (no longer than 15 minutes) at room temperature.

→ This created the permeability layer for the cellular membrane for the following immunostaining process.

3. After the fixation period, aspirated the PFA solution into the aspirator inside the chemical hood.
4. Rinsed each well with the warmed PBS three times. Swirled the PBS in the wells after each rinse and let it stand for 5-10 minutes between rinsing.
5. Wrapped the 12-well plate in the parafilm and left the devices in the PBS solution at 4 °C. (We recommend staining as soon as possible but can leave in this solution for several days if not staining immediately).

4.5 Fluorescent staining for cell morphologies

In order to observe cardiomyocyte morphologies and to also prove that the cells we used in our study are true cardiomyocytes, two parts of the cells were stained: 1) nucleus and 2) actin filament.

The following steps used in our staining process are as follows:

4.5.1 Nucleus

We took 1μl of DAPI (5.08741, Sigma) stock solution and diluted to a 200μl volume of PBS. We obtained a final concentration of 25ppm after adding the staining dye to the PBS mixture to obtain 200μl per device. The devices were placed face down in the liquid mixture. After all the devices were placed into the PBS and were stained, we covered the petri dish with aluminum foil to prevent cell exposure to light.

We then incubated the devices at room temperature for 1-2 hours. After this period, we moved the devices to a 12-well plate containing a PBS solution and rinsed each well with warmed PBS three times to remove unbounded DAPI conjugates. We then allowed the devices to sit in the PBS for 5-10 minutes between washes.

4.5.2 Actin filament

We added 1mL Dimethyl Sulfoxide(DMSO) (Sigma) to a Phalloidin, Fluorescein isothiocyanate labeled (P5282, Sigma) stock solution to yield a concentration of 1mg/mL.

Taking 1μl of the Phalloidin stock solution, we stained one drop to a 200μl volume of PBS. Each device then contained 200 μl of the stain and PBS mixture. We placed the devices face down in the liquid mixture. After the devices were all stained and placed in the PBS, they were placed inside a 35mm petri dish which contained DI water to prevent the cells from drying out. They were then covered with aluminum foil to prevent light from

entering the cells.

The petri dishes were incubated at room temperature overnight. After this period, the devices were moved to a 12-well plate containing a PBS solution. Each well was rinsed with warmed PBS three times to remove unbound Phalloidin conjugate. The devices were allowed to sit in the PBS solution for 5-10 minutes between washes.

Once all the staining steps were completed, we used two different methods to handle the imaging.

1. Mounted devices onto microscope slides.
    1) Prepared one microscope slide for each device
    2) Cleaned microscope slide and labeled with name, date, seeded date, fixed date, and cell type.
    3) Applied 1μl of Prolong Gold (S7114, Sigma), which is an anti-fade solution, onto the center of each slide.
    4) Remove the rinsed devices from the 12-well plate with PBS solution and use a Kimwipe towelette to dry.
    5) Once excess moisture was removed from the devices, gently placed the device cells facing downwards onto the Prolong Gold drop of one of the slides. To do this, first hold the device at a 45-degree angle (cell facing downwards) against the slide. Touch the edge of the drop with the edge of the device. Slowly lower the device onto the drop and gently press it against the slide. Make sure there are no bubbles between the device and slide.
    6) Cover with an opaque container (i.e. not clear/transparent) and incubate for at least 24 hours at room temperature.

7) After the 24-hour incubation period, seal a coverslip on top of each device with a glue gun.

8) Once dry, the slides can be used for imaging. If the slides are not imaged immediately, store the devices in a square petri dish and cover with aluminum foil and store in a -20 °C freezer.

2. Store all devices in the 12-well plate containing a 0.03% Sodium-Azide solution (Fisher Chemical)

1) Weigh 3mg of the Sodium-Azide stock powder.

2) Add 99.997g DI water to obtain a concentration of 0.03%.

3) Soak the devices in the 12-well plates with the Sodium-Azide solution to prevent mold from forming.

4) Wrap the 12-well plate in parafilm.

5) Store all 12-well plates in a polystyrene foam box and store the box at 4 °C under refrigeration for several days if not imaging immediately.

4.6 Microscope for cell imaging

An inverted microscope (IX51, Olympus) (Figure 4-4) was used to monitor the cell morphology.

To obtain the bright field images, a Sony/Nikon digital camera was attached to the microscope. After imaging, we uploaded the camera digital photos to a desktop computer. To obtain fluorescent images, we used a 4M-pixel Hamamatsu CCD camera on an Olympus IX51 inverted microscope for a very short period. All the devices that were mounted on the microscope slide were done with this CCD camera. Afterwards, we used Dr. Brewer's inverted microscope (BX51W1, Olympus) (Figure 4-5) to obtain more images. The

objective lens was allowed to touch the devices and were soaked in a petri dish filled with a PBS solution. The immersion of the lens in the liquid PBS reagent, allowed us to obtain better and clearer images. We found the main excitation/emission wavelengths were 350nm/460nm (DAPI), and 482nm/536nm Fluorescein isothiocyanate (FITC) for actin. We adjusted the contrast and brightness to eliminate the background using ImageJ software.

Figure 4-4. Image of inverted microscope used in this study.

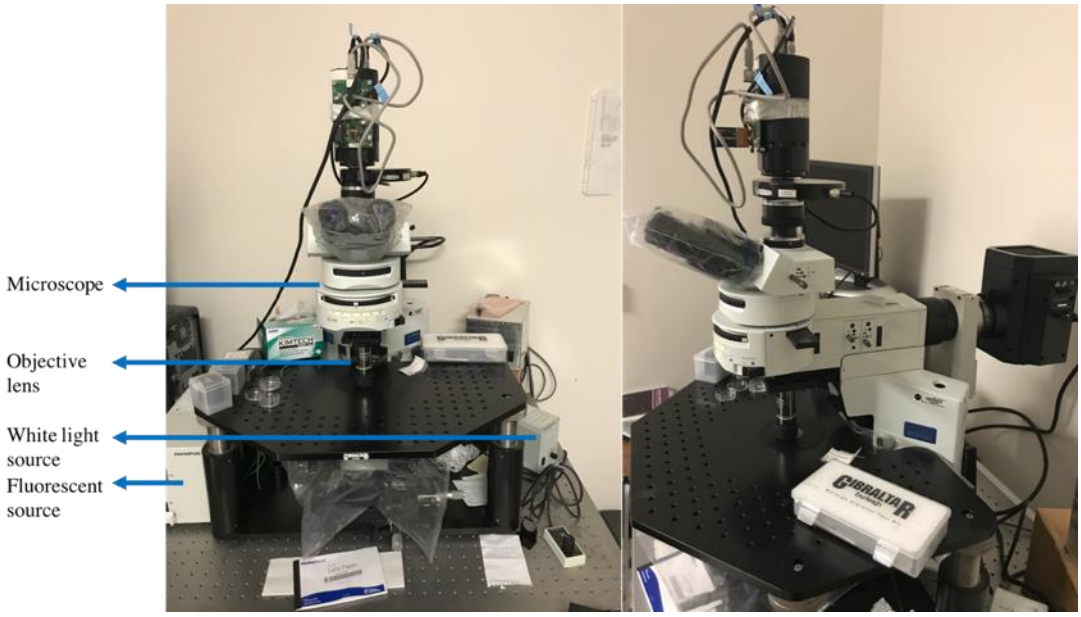

Figure 4-5. Images of the inverted microscope used to obtain the fluorescent images in this study.

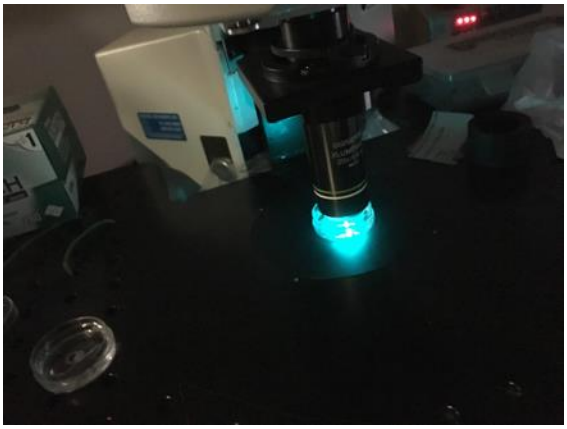

Figure 4-6. Image of the FITC fluorescent light.

4.7 Experimental results

4.7.1 Cellular alignment on micro-patterned PDMS

We found that the cell contracting phenomenon was not only in our 25T flask but also in our micro-patterned devices which we observed when it reached confluence, usually seen

on Day 2.

In our experimental set-up, micron-sized ridges and grooves on the SU-8 mold were fabricated using standard photolithographic techniques. Given that the average measured size of the HL-1 cardiomyocyte was approximately 10~25µm [47], we hypothesized that HL-1 cells will demonstrate greater alignment upon receiving the most mechanical support at 25µm dimensions. From the experimental results, we found that the cells have the best alignment with a 20µm pattern.

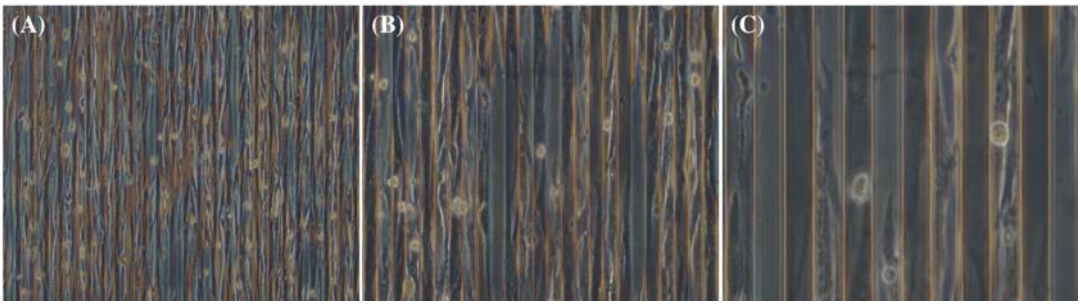

Figure 4-7. Neonatal rat ventricular myocyte (NRVM)cells were seeded on 20 µm x 20µm micro-patterned platform on Day 3. Cell density was $1.6x10^5$ per device: (A) 10X magnification, (B) 20X magnification and (C) 40X magnification.

4.7.2 Immunostaining results of cardiac cells

Fluorescent images of cardiomyocytes on Day-3 culture are shown in Figure XX. The primary antibodies used for staining included DAPI to observe the nuclei and Phalloidin to examine the actin within the cardiomyocyte.

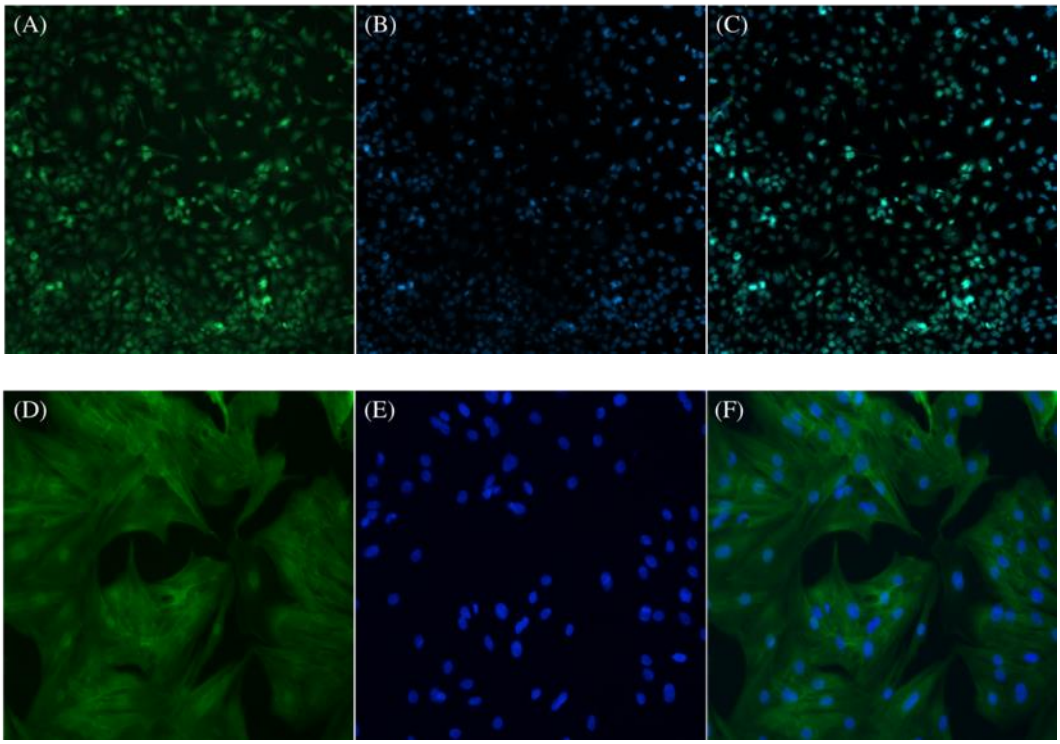

Figure 4-8. (A)HL-1 cells cultured for 3 days on (e.g. cells seeded on blank PDMS): (A) staining phalloidin to observe actin of the HL-1, (B) staining DAPI to observe the HL-1nuclei, and (C) merging actin and DAPI. (20X magnification). Neonatal rat ventricular myocyte (NRVM) cells cultured for 3 days (e.g. cells seeded on blank PDMS): (D) staining phalloidin to observe actin of the NRVM, (E) staining DAPI to observe the NRVM nuclei, and (F) merging actin and DAPI. (20X magnification)

4.7.3 Orientation analysis

An orientation analysis was conducted using image processing routines in MATLAB and ImageJ. Raw images were captured with a 4M-pixel Hamamatsu CCD camera mounted onto an Olympus IX51 inverted microscope. The patterned grooves from the bright field images were aligned vertically, which were then cropped to 850 x 700 pixels. All the images were automatically adjusted for brightness/contrast and the bandpass was filtered to 40-3 pixels to correct for noise. To capture the cells outlines, all the images were binarized and each of the outlines were fitted to an elliptical shape with circularity between

15 - 80%. The ellipses which contained data outside this range or with an area less than 10 pixels were eliminated to ensure that the ridges/grooves were not processed during analysis (Figure 4-9).

The experiments were conducted after the third day of the seeding. We used a sample size of 50 (5, 10, 15, 20, 30) patterned devices per day. We thus created 150 possible patterned data points (3*50) and 10 control/non-patterned data points.

Two parameters were investigated to quantify the orientation: (1) percent oriented cells and (2) ratio of the major/minor axis of the fitted ellipses. A cell with a fitted ellipse that aligned perfectly vertically (with the direction of the ridges) was assigned 90 degrees. Any cell within the range of 75 degrees to 105 degrees was considered aligned. The percentage of all cells considered aligned constituted the first parameter. The ratio of the major/minor axis was to use to further quantify the alignment since a more elongated cell body would be more prominently aligned. In summary, all five versions of the PDMS devices showed increased orientation with an average showing 56% with those possessing 20μm exhibiting the most significant results.

We found that the average control or non-orientation was found to be 12% while the average patterned orientation was calculated to be 68%. This can be seen graphically in Figure 4-9 and Figure 4-10. Results obtained from the quantification of the cellular alignment from MATLAB. Use 20μm group as example shown here. (A) shows a non-patterned control environment with average angle orientation of 103 degrees; we can see this is due to random orientation across all cells. Right side (B-F) shows the micro-patterned device which shows the majority of cells aligned at or around 90 degrees. (B) 20μm x 5μm. (C) 20μm x 10μm. (D) 20μm x 15μm. (E) 20μm x 20μm. (F) 20μm x 30μm.

From these polar charts, we can see that 15μm and 20μm has better alignment for cardiomyocytes. Furthermore, we found that the major/minor axis ratio was found to be visually higher with the variable group with a statistical analysis to be determined. Among all the testing parameters, those found to be in the range of 15-20μm for the micron ridge length, had on average a higher percent orientation ~5% and had a visually greater major/minor axis.

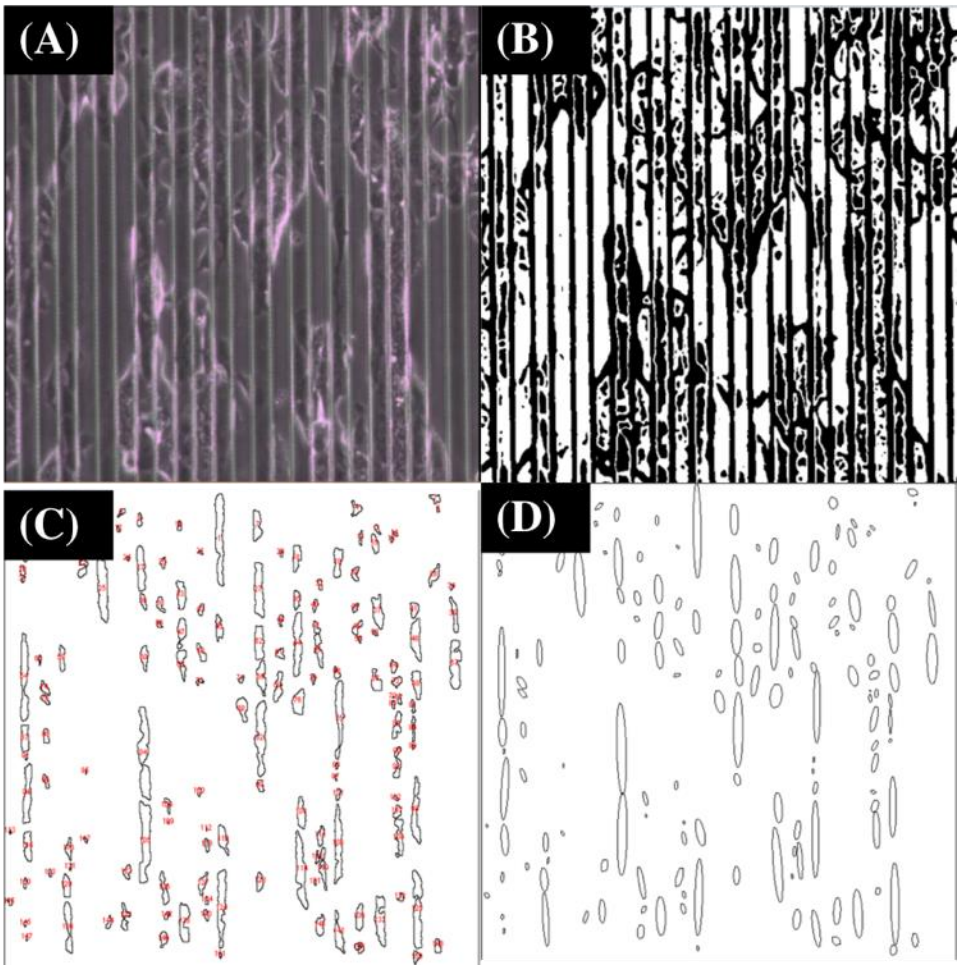

Figure 4-9. (A) Original image on Day 2 after original seeding of cardiomyocytes onto the 20μm x 20μm micro-pattern and before processing. (B) Completed binarization from ImageJ showing the outlines of the cellular membranes. (C) Cellular outlines from automatic particle analysis algorithm from ImageJ. (D) Elliptical fitting to the outlines generated which were used to assign orientation angle and area.

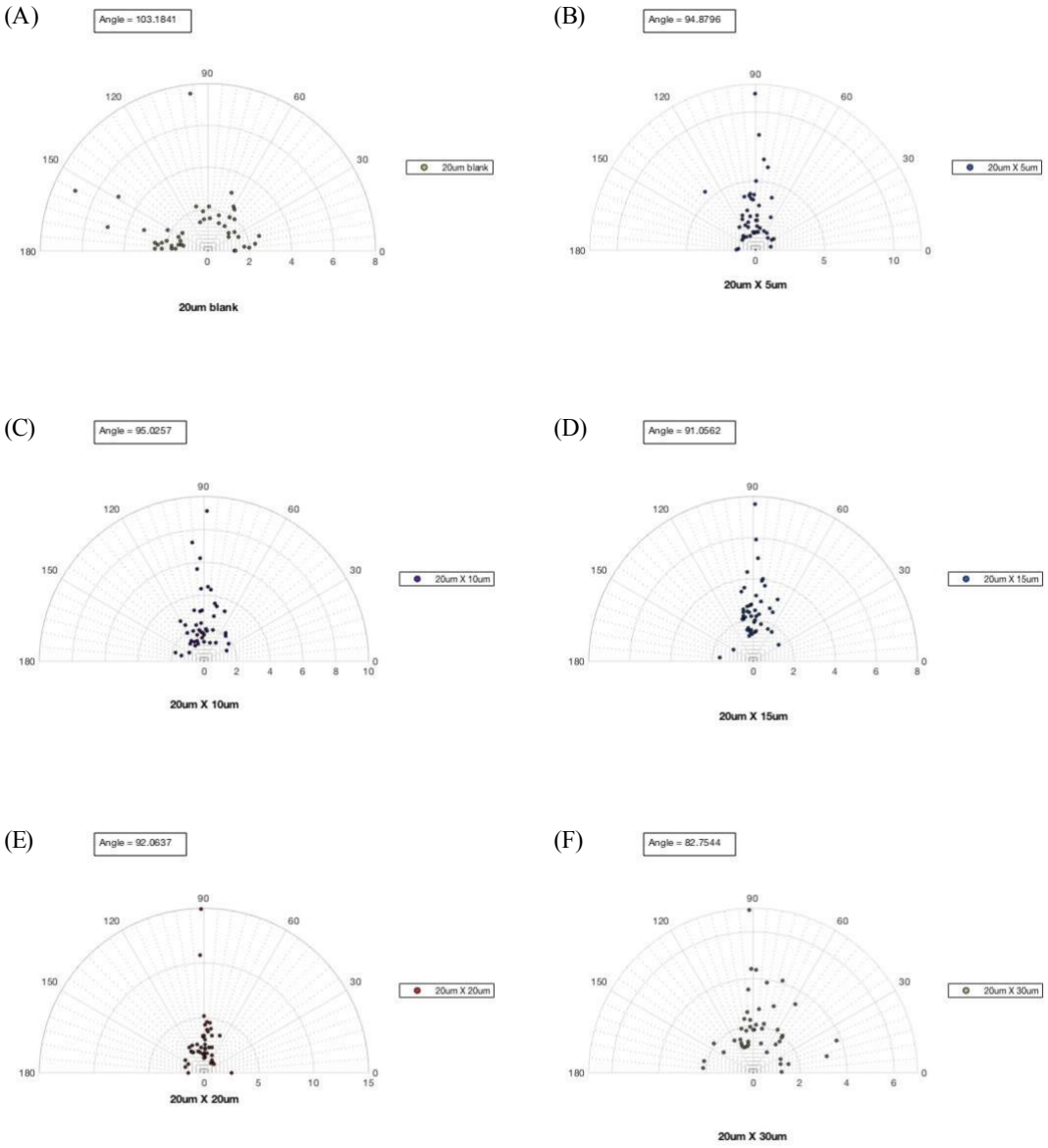

Figure 4-10. Results obtained from the quantification of the cellular alignment from MATLAB. Use 20µm group as example shown here. (A) shows a non-patterned control environment with average angle orientation of 103 degrees; we can see this is due to random orientation across all cells. Right side (B-F) shows the micro-patterned device which shows the majority of cells aligned at or around 90 degrees. (B) 20µm x 5µm. (C) 20µm x 10µm. (D) 20µm x 15µm. (E) 20µm x 20µm. (F) 20µm x 30µm. From these polar charts, we can see that 15µm and 20µm has better alignment for cardiomyocytes.

Chapter 5 CONCLUSIONS AND FUTURE WORK

5.1 Conclusions

In this study, a new platform was developed to have cardiomyocytes align in a proper direction so that we can adopt for further cardiac drug screening. The alignment of cardiomyocytes was achieved by creating PDMS-based surface microstructures with various grooves using a MEMS processes. Through a series of detailed experimental works, the pros-and-cons of different parameters including HL-1 cardiomyocytes versus primary mice cardiomyocytes, as well as the proper cell density to be seeded onto grooves of various widths, etc., have been examined in detail.

Using the results obtained in this thesis, a platform with a potential to facilitate drug screening, testing, etc., related to cardiovascular diseases can be confirmed to have achieved initial success. Furthermore, it should be noted that the emphasis of this thesis was to study the interaction of cardiomyocytes and micro-surface structures so that we can identify the parameters important to applications such as for drug screening, diagnostics, testing, etc. From the results obtained, recent advancements such as 3D printing or laser micro-machining to create micro-surface structures, can certainly be adopted to further advance our knowledge and to speed up drug development times for more medical related research.

5.2 Future Works

With the findings of this study, we now have enough understanding to look further to understand the effects from three additional primary variables which were previously assumed to be constant or negligible in prior studies. These variables include: cell density,

cardiomyocyte type, and topology height. Each variable is described below.

5.2.1 Cell Density

A point of discussion arose after we attempted to seed the cardiomyocytes onto the micro-patterns to achieve doubling of the cell density after seeding. It was noted after three days of culturing that an increased cell density lead to a decrease in cellular alignment. We believe there may be multiple factors which led us to the conclusion that an increased cellular density can lead to an increased mechanical stress between the cells and that the prolific number of stressed cells will not enable proper seeding onto the micro-pattern devices. In our work, we seeded $3.7x10^5$/mL for each device. However, when we tried to obtain double density seeding once on a device, we found that the cell alignment was impaired after three days of cell growth. In addition, the device with the double cell density seeding was more difficult to analyze using the image processing techniques we adopted in this study. We conjecture that too many cells will create too much stress between the cells to allow for natural growth of the cells.

To test the above-mentioned hypothesis and to further study the effect of cell density on our newly developed platform, grooves with 5 different widths (5μm, 10μm,15μm, 20μm, 30μm) was chosen as the experimental groups in addition to one black PDMS device as the control. All of the devices were seeded with half of the cell density, i.e., $1.85x10^5$/mL for each device. These five experimental groups and the control were examined after seeding with half the cell density for three days. The morphology was observed using MATLAB and the data was processed similarly to procedures in prior works.

5.2.2 Primary vs. HL-1 Cardiomyocytes

One of the assumptions made during the prior experimental procedures held that HL-1 cardiomyocyte cells would be equivalent to primary mouse cardiomyocyte cells in its morphology. To validate this assumption, the same tests were conducted in the same way as previous studies. That is, the seeding of cells onto 5um, 10um, 15um, 20um, and 30um was used for comparison and the experimental data obtained was analyzed. Even though some primary mice cardiomyocytes were used in this study, more sample numbers can be adopted to repeat the experiments. If the exact experimental results obtained are the same as we have obtained for HL-1 cells, it validates and confirms that this new platform can work for real cardiomyocytes.

5.2.3 Topology Height

The average cardiomyocyte dimensions have been cited to be approximately 130μm to140μm in length, 17μm in width, and 6μm in height [48][49][50]. Currently, we incorporated into our experiments with 5μm topological grooves, thus supporting approximately 83% of the cardiomyocyte volume within its ridges. The question we seek to answer is how much height support is needed until the cardiomyocytes no longer display uniform alignment or if taller structures can better align the cells. To test the above-mentioned hypothesis, grooves of 2μm and 10μm dimensioned heights coupled with the dimensions adopted in this thesis, i.e., (5μm,10μm,15μm, 20μm, 30μm) were tested and the data obtained comparatively analyzed.

In the following phases of further suggested study, we can integrate this platform with a piezoelectric transducer layer so as to measure the cardiomyocyte contractile forces in-situ. In such a case, we can focus on using primary cells as the experimental model since

they can generate higher contract stresses when compared to cell lines while they are fresh. Another advantage lies on the fact that primary cells are closer to real cardiomyocytes. To further advance this particular line of study, our long-term goal would be to use an automatic monitoring system for monitoring cardiac cells.

Appendix References

[1] S. Carter, “Haptotactic islands,” Exp. Cell Res., vol. 48, no. 1, pp. 189–193, 1967.

[2] G. S. Ferguson, M. K. Chaudhury, H. A. Biebuyck, and G. M. Whitesides, “Monolayers on disordered substrates: self-assembly of alkyltrichlorosilanes on surface-modified polyethylene and poly(dimethylsiloxane),” *Macromolecules*, vol. 26, no. 22, pp. 5870–5875, 1993.

[3] S. H. Park, J. W. Hong, J. H. Shin, and D.-Y. Yang, “Quantitatively Controlled Fabrication of Uniaxially Aligned Nanofibrous Scaffold for Cell Adhesion,” *J. Nanometer.*, vol. 2011, pp. 1–9, 2011.

[4] M. Marelli, N. Gadhari, G. Boero, M. Chiquet, and J. Brugger, “Cell force measurements in 3D microfabricated environments based on compliant cantilevers,” *Lab Chip*, vol. 14, no. 2, pp. 286–293, 2014.

[5] Y. Morimoto, S. Mori, F. Sakai, and S. Takeuchi, “Human induced pluripotent stem cell-derived fiber-shaped cardiac tissue on a chip,” *Lab Chip*, vol. 16, no. 12, pp. 2295–2301, 2016.

[6] P. Linder et al., “Contractile tension and beating rates of self-exciting monolayers and 3D-tissue constructs of neonatal rat cardiomyocyte cells,” *Med. Biol. Eng. Comput.*, vol. 48, no. 1, pp. 59–65, 2009.

[7] M. L. Rodriguez, B. T. Graham, L. M. Pabon, S. J. Han, C. E. Murry, and N. J. Sniadecki, “Measuring the Contractile Forces of Human Induced Pluripotent Stem Cell-Derived Cardiomyocyte cells With Arrays of Microposts,” *J. Biomech. Eng.*, vol. 136, no. 5, p. 051005, Oct. 2014.

[8] G. Laroche et al., “Polyvinylidene fluoride (PVDF) as a biomaterial: From polymeric

raw material to monofilament vascular suture," *J. Biomed. Mater. Res.*, vol. 29, no. 12, pp. 1525–1536, 1995.

[9] A. Grosberg et al., "Self-Organization of Muscle Cell Structure and Function," *PLoS Comput. Biol.*, vol. 7, no. 2, 2011.

[10] "Pharmaceutical Research and Manufacturers of America," *Phrma*. [Online]. Available: http://www.phrma.org/. [Accessed: 01-Jun-2018].

[11] N. Uberoi and J. Cohen. "Expenditures for Heart Disease among Adults Age 18 and Older: Estimates for the U.S. Civilian Noninstitutionalized Population, 2009, Statistical Brief #388. Internet: http://meps.ahrq.gov/mepsweb/data_files/publications/st393/stat393.shtml, Oct., 2012. [Accessed: 01-Jun-2018].

[12] "Emerging Therapeutic Company Investment and Deal Trends." [Online]. Available: https://www.bio.org/sites/default/files/BIO_Emerging_Therapeutic_Company_Report_2006_2015_Final.pdf. [Accessed: 01-Jun-2018]..

[13] "Cardiovascular diseases (CVDs)," *World Health Organization*. [Online]. Available: http://www.who.int/mediacentre/factsheets/fs317/en. [Accessed: 01-Jun-2018].

[14] "Division for Heart Disease and Stroke Prevention," *Centers for Disease Control and Prevention*, 23-Aug-2017. [Online]. Available: http://www.cdc.gov/dhdsp/data_statistics/fact_sheets/fs_heart_disease.htm. [Accessed: 01-Jun-2018].

[15] D.-H. Kim et al., "Nanoscale cues regulate the structure and function of macroscopic cardiac tissue constructs," *Proc. Natl. Acad. Sci. U S A*, vol. 107, no. 2, pp. 565–570, 2009.

[16] A. Grosberg, P. W. Alford, M. L. McCain, and K. K. Parker, “Ensembles of engineered cardiac tissues for physiological and pharmacological study: Heart on a chip,” *Lab Chip*, vol. 11, no. 24, p. 4165, 2011.

[17] Y. Shin et al., “Microfluidic assay for simultaneous culture of multiple cell types on surfaces or within hydrogels,” *Nat. Protoc.*, vol. 7, no. 7, pp. 1247–1259, Jul. 2012.

[18] *Soft Lithography Fabrication-New Shared Experimental Facility - Materials Research Science and Engineering Center at Harvard*. [Online]. Available: https://www.mrsec.harvard.edu/research/nugget_84.php. [Accessed: 01-Jun-2018].

[19] “SU-8 3000 Data Sheet ver 4.2 - MicroChem.” [Online]. Available: http://microchem.com/pdf/SU-8 3000 Data Sheet.pdf. [Accessed: 01-Jun-2018].

[20] M. J. Madou, *Fundamentals of microfabrication and nanotechnology*. Boca Raton, FL: CRC Press, 2012.

[21] Y. Xia and G. M. Whitesides, “Softlithographie,” *Angewandte Chemie*, vol. 110, no. 5, pp. 568–594, Feb. 1998.

[22] D. Qin, Y. Xia, and G. M. Whitesides, “Rapid prototyping of complex structures with feature sizes larger than 20 um,” *Adv. Mater.*, vol. 8, no. 11, pp. 917–919, 1996.

[23] W. C. Claycomb et al., “HL-1 cells: A cardiac muscle cell line that contracts and retains phenotypic characteristics of the adult cardiomyocyte,” *Proc. Natl. Acad. Sci. U S A*, vol. 95, no. 6, pp. 2979–2984, 1998.

[24] S. N. Bhatia and D. E. Ingber, “Microfluidic organs-on-chips,” *Nature Biotechnology*, vol. 32, no. 8, pp. 760–772, 2014.

[25] W.-H. Zimmermann, “Tissue Engineering of a Differentiated Cardiac Muscle Construct,” *Circ. Res.,* vol. 90, no. 2, pp. 223–230, 2001.

[26] S. D. Lundy, W.-Z. Zhu, M. Regnier, and M. A. Laflamme, "Structural and Functional Maturation of Cardiomyocytes Derived from Human Pluripotent Stem Cells," *Stem Cells Dev.*, vol. 22, no. 14, pp. 1991–2002, 2013.

[27] I. P. Herman, *Physics of the human body*. Berlin: Springer, 2007.

[28] G. Bergtrom, *Cell and Molecular Biology 2e: What We Know & How We Found Out*. Biological Sciences Faculty Books, 2016.

[29] A. Salameh et al., "Cyclic Mechanical Stretch Induces Cardiomyocyte Orientation and Polarization of the Gap Junction Protein Connexin43," *Circ. Res.*, vol. 106, no. 10, pp. 1592–1602, Aug. 2010.

[30] A. J. Shanker, "Matrix Protein-Specific Regulation of Cx43 Expression in Cardiac Myocytes Subjected to Mechanical Load," *Circ. Res.*, vol. 96, no. 5, pp. 558–566, 2005.

[31] G. Kensah et al., "A Novel Miniaturized Multimodal Bioreactor for Continuous InSitu Assessment of Bioartificial Cardiac Tissue During Stimulation and Maturation," *Tissue Eng. Part C Methods*, vol. 17, no. 4, pp. 463–473, 2011.

[32] N. L. Tulloch et al., "Growth of Engineered Human Myocardium With Mechanical Loading and Vascular Coculture," *Circ. Res.*, vol. 109, no. 1, pp. 47–59, 2011.

[33] T.-L. Wang, Y.-Z. Tseng, and H. Chang, "Regulation of Connexin 43 Gene Expression by Cyclical Mechanical Stretch in Neonatal Rat Cardiomyocyte cells," *Biochem. Biophys. Res. Commun.*, vol. 280, no. 2, p. 588, 2001.

[34] E. Holt, P. K. Lunde, O. M. Sejersted, and G. Christensen, "Electrical stimulation of adult rat cardiomyocyte cells in culture improves contractile properties and is associated with altered calcium handling," *Basic Res. Cardiol.*, vol. 92, no. 5, pp. 289–

298, Jan. 1997.

[35] Y.-C. Chan et al., “Electrical Stimulation Promotes Maturation of Cardiomyocyte cells Derived from Human Embryonic Stem Cells,” *J. Cardiovasc. Transl. Res.,* vol. 6, no. 6, pp. 989–999, Jan. 2013.

[36] M. Radisic et al., “Functional assembly of engineered myocardium by electrical stimulation of cardiac myocytes cultured on scaffolds,” *Proc. Natl. Acad. Sci. U S A,* vol. 101, no. 52, pp. 18129–18134, 2004.

[37] T. B. Johnson, R. L. Kent, B. A. Bubolz, and P. J. McDermott, “Electrical stimulation of contractile activity accelerates growth of cultured neonatal cardiomyocytes,” *Circ. Res.*, vol. 74, no. 3, pp. 448–459, Jan. 1994.

[38] Y. Xiao et al., “Microfabricated perfusable cardiac biowire: a platform that mimics native cardiac bundle,” *Lab Chip*, vol. 14, no. 5, pp. 869–882, 2014.

[39] S. S. Nunes et al., “Biowire: a platform for maturation of human pluripotent stem cell–derived cardiomyocyte cells,” *Nat. Methods*, vol. 10, no. 8, pp. 781–787, 2013.

[40] J. Kim et al., “Quantitative evaluation of cardiomyocyte contractility in a 3D microenvironment,” *J. Biomech.,* vol. 41, no. 11, pp. 2396–2401, 2008.

[41] A. W. Feinberg et al., “Controlling the contractile strength of engineered cardiac muscle by hierarchal tissue architecture,” *Biomaterials*, vol. 33, no. 23, pp. 5732–5741, 2012.

[42] F. Y. McWhorter, T. Wang, P. Nguyen, T. Chung, and W. F. Liu, “Modulation of macrophage phenotype by cell shape,” *Proc. Natl. Acad. Sci. U S A*, vol. 110, no. 43, pp. 17253–17258, Jul. 2013.

[43] S. M. White, P. E. Constantin, and W. C. Claycomb, “Cardiac physiology at the

cellular level: use of cultured HL-1 cardiomyocyte cells for studies of cardiac muscle cell structure and function," *Am. J. Physiol. Heart Circ. Physiol.*, vol. 286, no. 3, 2004.

[44] P. Sreejit, S. Kumar, and R. S. Verma, "An improved protocol for primary culture of cardiomyocyte from neonatal mice," *In Vitro Cell Dev. Biol. Anim.*, vol. 44, no. 3-4, pp. 45–50, 2008.

[45] P. W. Alford, A. W. Feinberg, S. P. Sheehy, and K. K. Parker, "Biohybrid thin films for measuring contractility in engineered cardiovascular muscle," *Biomaterials*, vol. 31, no. 13, pp. 3613–3621, 2010.

[46] A.C. Baker, "Fabrication of Micro-Platforms for Studying the Biomechanics of Cardiomyocyte cells", M.S. Thesis, University of California, Irvine, USA, 2013.

[47] K. A. Nibbelink, D. X. Tishkoff, S. D. Hershey, A. Rahman, and R. U. Simpson, "1,25(OH)2-vitamin D3 actions on cell proliferation, size, gene expression, and receptor localization, in the HL-1 cardiac myocyte," *J. Steroid Biochem. Mol. Biol.*, vol. 103, no. 3-5, pp. 533–537, 2007.

[48] S. Melo et al., "Resistance Training Regulates Cardiac Function through Modulation of miRNA-214," *Int. J. Mol. Sci.*, vol. 16, no. 12, pp. 6855–6867, 2015.

[49] R. E. Tracy and G. E. Sander, "Histologically Measured Cardiomyocyte Hypertrophy Correlates with Body Height as Strongly as with Body Mass Index," *Cardiol. Res. Pract.*, vol. 2011, pp. 1–9, 2011.

[50] A. Gerdes and J. Capasso, "Structural remodeling and mechanical dysfunction of cardiac myocytes in heart failure," *J. Mol. Cell. Cardiol.*, vol. 27, no. 3, pp. 849–856, 1995.